Metabolic Dependency Shapes Bivalent Antiviral Response in Host Cells in response to poly:IC: The Role of Glutamine

Grégorie Lebeau[1,2]*, Aurélie Paulo-Ramos[2], Mathilde Hoarau[2], Daed El Safadi[1], Olivier Meilhac[2], Pascale Krejbich-Trotot[1], Marjolaine Roche[1] and Wildriss Viranaicken[1,2]*

[1] Université de la Réunion, INSERM U1187, CNRS UMR 9192, IRD UMR 249, Unité Mixte Processus Infectieux en Milieu Insulaire Tropical, Plateforme Technologique CYROI, 94791 Sainte Clotilde, La Réunion, France

[2] Université de La Réunion, INSERM, UMR 1188 Diabète athérothombose Réunion Océan Indien (DéTROI), Campus Santé Université de la Réunion, 77 avenue du Docteur Jean-Marie Dambreville, 97410 Saint-Pierre, France

* Correspondence: gregorie.lebeau@univ-reunion.fr (G.L.); wildriss.viranaicken@univ-reunion.fr

Abstract: The establishment of effective antiviral responses within host cells is intricately related to their metabolic status, shedding light on immunometabolism. In this study, we investigated the hypothesis that cellular reliance on glutamine metabolism contributes to the development of a potent antiviral response. We evaluated the antiviral response in the presence or absence of L-glutamine in the culture medium, revealing a bivalent response hinging on cellular metabolism. While certain interferon-stimulated genes (ISGs) exhibited higher expression in an oxidative phosphorylation (OXPHOS)-dependent manner, others were surprisingly upregulated in a glycolytic-dependent manner. This metabolic dichotomy was influenced in part by variations in IFN-β expression. We initially demonstrated that the presence of L-glutamine induced an enhancement of OXPHOS in A549 cells. Furthermore, in cells either stimulated poly:IC or infected with Dengue Virus and Zika Virus, a marked increase in ISGs expression was observed in a dose-dependent manner with L-glutamine supplementation. Interestingly, our findings unveiled a metabolic dependency in the expression of specific ISGs. In particular, genes such as ISG54, ISG12 and ISG15 exhibited heightened expression in cells cultured with L-glutamine, corresponding to higher OXPHOS rates and IFN-β signaling. Conversely, the expression of viperin and 2'-5'-oligoadenylate synthetase 1 was inversely related to L-glutamine concentration, suggesting a glycolysis-dependent regulation, confirmed by inhibition experiments. This study highlights the intricate interplay between cellular metabolism, especially glutaminergic and glycolytic, and the establishment of the canonical antiviral response characterized by the expression of antiviral effectors, potentially paving the way for novel strategies to modulate antiviral responses through metabolic interventions.

Keywords: antiviral response, OXPHOS, mitochondrial respiration, glycolysis, metabolic reprogramming, immunometabolism

Abbreviations

2-DG	2-deoxyglucose
A549^{Dual}	A549-Dual™, expressing NF-κB-SEAP and IRF-Luc reporters
GAS	Gamma interferon activation site
IFN	Interferon
IFNAR	IFNs α/β receptor
IRF	Interferon Regulatory Factor
ISG	Interferon Stimulated Gene
ISRE	IFN-stimulated response element
mROS	Mitochondrial reactive oxygen species
OXPHOS	Oxidative phosphorylation
PIC	Poly(I:C) (HMW) / LyoVec™

1. Introduction

Over the past two decades, we have been regularly confronted with our vulnerability to infectious diseases, whether emerging or re-emerging [1–7]. To deal with epidemics that can take on worldwide proportions, major research efforts have been required to gain a better understanding, not only of the emergence of these viruses, but also the pathophysiology associated with them. The antiviral response is one of the most widely explored aspects, depicting the host-pathogen relationship that develops during infection, which represents an evolutionary mechanism elaborated by the host to struggle against viral infections [8]. The canonical pathway of the antiviral response - the Interferon (IFN) pathway - is initiated by the recognition of pattern associated molecular patterns (PAMPs), usually viral nucleic acids, by pattern recognition receptors (PRRs). The viral genome released into the cytosol is specifically recognized by RIG-I like receptors (RLR *e.g.,* RIG-I and MDA5) notably for viral 5'PPP-RNA and cyclic GMP-AMP Synthase (cGAS) for viral dsDNA [9,10]. Nucleic acids of endosomal origin are recognized by Toll-like receptors (TLRs) found in the endosome; TLR3 for dsRNA, TLR7/8 for ssRNA and TLR9 for DNA containing unmethylated CpGs [9]. Most of these receptors activate interferon regulatory factors (IRFs) via adaptor proteins. For example, RIG-I and MDA5 interact with MAVS via their CARD domain, leading to a signaling cascade involving TRAF3, TBK1 and IKKε, resulting in phosphorylation and heterodimerization of IRF7 and IRF3 [9]. Similarly, TLR3, via TRIF, leads to activation of IRF3 and 7 while TLR7, 8 and 9, via MYD88, lead to the formation of IRF7 homodimers [9]. More recently, the demonstration of the ability of cGAS to produce cyclic GMP-AMP (cGAMP) following the detection of cytosolic dsDNA led to the description of a new IFN production pathway, via the Stimulator of Interferon Genes – STING [10]. STING, through TBK1, leads to phosphorylation and homodimerization of IRF3 [10]. Finally, IRFs activated by these different pathways can translocate to the nucleus of the infected cell, where they interact with their promoter to allow transcription of type I and III IFNs. It is difficult to distinguish the intrinsic activity of type I IFNs (predominantly β) from type III IFNs, as their secretion occurs concomitantly [11]. Secreted IFNs act in an autocrine and paracrine manner, via their IFNAR1/2 and IFNLR1/IL-10Rβ receptors respectively, leading to the phosphorylation and homodimerization of STAT1 (GAF) on the one hand and, on the other, to the formation of the ISGF3 complex, composed of IRF9 and phosphorylated STAT1 and 2 [11,12]. ISGF3 interacts with the interferon-sensitive responsive element (ISRE), while GAF interacts with the gamma interferon activation site (GAS), in both cases leading to the expression of ISGs [11,12]. Alternatively, specific antiviral programs have been demonstrated, involving, for example, peroxisomal localization of MAVS which, after interaction with RIG-I, specifically induces activation of IRF1 leading to direct expression of antiviral genes and, at epithelial level, IFN-λ [13,14]. The interferon-stimulated genes (ISGs) encode antiviral proteins that have various functions on the virus life cycle, including inhibition of viral entry (myxovirus resistance genes), translation and replication (IFIT family, viperin), or even budding (tetherin) [11]. Additionally, they are able to improve sensing or potentiate interferon signaling pathways [15].

The IFN response is acute, representing the first line of defense deployed by cells at the site of infection, limiting the spread of the virus throughout the body. It also enables the innate and adaptive immune responses to be established accordingly [16]. However, this line of defense is vulnerable and many viruses have developed mechanisms to circumvent and control the antiviral response. To avoid the IFN response, several of these mechanisms are often active simultaneously. Upstream of IFN secretion, certain viruses appear to act by limiting the detection of their genome or by interfering with the signaling pathways leading to IFN secretion. For example, the N and NSP5 proteins of

78 SARS-CoV-2 limit the polyubiquitination of RIG-I, which is involved in the stabilization of its CARD domains and the
79 aggregation of MAVS [17]. Viral protease from HCV has shown the ability to cleave Cardif an adaptor protein in the RIG-
80 I antiviral pathway [18]. Viral escape can also occur downstream of IFN secretion by inhibiting ISG production. Many
81 viruses (*e.g.,* Nipah virus, Measles virus, DENV, ZIKV) are able to target STAT1 and STAT2, sequestering them or causing
82 their degradation [19]. Furthermore, while metabolism has proven to be of interest in the activation of immune cells
83 [20], it is no less central to the IFN response. Metabolism is a crucial control point for the virus during infection in
84 several regards. Firstly, during infection, the diversion of cellular metabolism from OXPHOS to glycolysis, via a Warburg-
85 like effect, allows the virus to access a quantity of biomass consistent with viral progeny [21]. On the other hand,
86 control of metabolism could limit its effects on the establishment of the antiviral response. Indeed, we have previously
87 shown that induction of the antiviral response by poly:IC in galactose-cultured cells, to boost their OXPHOS, resulted in
88 greater expression of ISGs than when cells based their metabolism on glucose use and glycolysis [22]. Consistent with
89 our results, mitochondrial ROS production was previously shown to induce MAVS oligomerization and type I IFN
90 production [23]. In support of this hypothesis, it was shown that cells resistant to HIV-induced aerobic glycolysis have a
91 higher antiviral potential and are accompanied by virus control [24]. Strengthening the link between cell respiration and
92 virus infection, flavivirus affects the respiratory pathways of infected cells, notably through inhibition of mitochondrial
93 fission by NS4B, which prevents the onset of mitochondrial antiviral status due to decreased ROS production [25,26].
94 Additionally, illustrating the deleterious effect of aerobic glycolysis on infected cells, the lactate produced by this
95 process has been shown to affect RIG-I-dependent IFN production by regulating MAVS [27].
96 It has been stated on several occasions that the supply of TCA and therefore of OXPHOS can occur through the
97 anaplerotic use of glutamine to give α-ketoglutarate. However, to date, the beneficial effect of glutamine during
98 infection remained unclear. Indeed, it has been suggested that infected cells may be 'addicted' to glutamine, although it
99 has not been established whether this addiction is due to the virus or rather to the requirement for glutamine to mount
100 an effective antiviral response [28]. The work of Shiratori et al. illustrates that the use of galactose to force the
101 metabolic reprogramming of cancer cells toward OXPHOS relies on increasing the glutamine pool to anaplerotically
102 generate TCA intermediates [29]. In light of these data and our previous work, we hypothesize here that the host cell
103 depends on glutamine to establish a metabolic process adapted to the development of an effective antiviral response.
104 To test this hypothesis, we decided to evaluate the antiviral response in the presence or absence of L-glutamine in the
105 culture medium. Interestingly, we demonstrated the existence of a bivalent antiviral response depending on cellular
106 metabolism. Indeed, some ISGs are more expressed in an OXPHOS-dependent manner, as we expected, while others
107 are more expressed in a glycolytic-dependent manner, the dichotomy in part relying on a variation of IFN-β expression.

108 **2. Materials and methods**

109 *2.1. Cells, viruses and reagents*

110 The human A549-Dual™ ($A549^{Dual}$) are adherent epithelial cells derived from A549 lung carcinoma cell line (ATCC,
111 CCL-185™). $A549^{Dual}$ were purchased from InvivoGen (ref. a549d-nfis, San Diego, CA, USA). Zika Virus (PF-25013-18) and
112 Dengue Virus serotype 2 (UVE/DENV-2/UNK/RE/CNR 14445) were amplified on Vero cells (ATCC, CCL-81) and viral titers
113 were determined by a standard plaque-forming assay as previously described with minor modifications [30]. QUANTI-
114 Luc™ substrate was obtained from InvivoGen (ref. rep-qlc1, San Diego, CA, USA). Oligomycin (ref. 75351), myxothiazol
115 (ref. T5580), 2-deoxyglucose (2-DG, ref. D8375), 2,4-dinitrophenol (DNP, ref. D198501) and rotenone (ref. R8875) was

purchased from Sigma-Aldrich (Saint-Louis, MO, USA). Poly(I:C) (HMW) / LyoVec™ (PIC) was purchased from InvivoGen (ref. tlrl-piclv, San Diego, CA, USA). MitoSOX™ Red was purchased from InvitroGen (ref. M36008, Carlsbad, CA, USA). Non-essential amino acid solution was purchased from PAN Biotech (ref. P08-32100, Aidenbach, Germany).

2.2. Cell culture

A549^{Dual} cells were cultured for maintenance at 37°C under a 5% CO_2 atmosphere in 4,5 g·L^{-1} glucose Dubecco's Modified Eagle's Medium – DMEM (PAN Biotech, Aidenbach, Germany) supplemented with 10% of heat-inactivated fetal bovine serum (FBS, Dutscher, Brumath, France), 100 U·mL^{-1} penicillin, 100 µg·mL^{-1} streptomycin, 2 mM L-glutamine and 0.5 µg·mL^{-1} amphotericin B (PAN Biotech, Dutsher, Brumath, France) and containing 10 µg·mL^{-1} blasticidin and 100 µg·mL^{-1} zeocin (InvivoGen, San Diego, CA, USA), for selection of cells expressing NF-κB-SEAP and IRF-Luc reporters.

2.3. Oxygen consumption rate assessment

A549^{Dual} cells were cultured in 25 cm^2 flasks, DMEM 4.5 g·L^{-1} glucose was replaced by RPMI 2 g·L^{-1} glucose, supplemented or not with 2 mM L-glutamine, either containing PIC or not, 24 hours before oxygen consumption rate (OCR) assessment. The cells were then washed with PBS, collected with trypsin / EDTA, and centrifuged at 800×*g* for 5 min, at room temperature. Subsequently, cell pellets were suspended in a volume of RPMI 2 g·L^{-1} glucose, supplemented or not with 2 mM L-glutamine, allowing the number of cells per chamber to be standardized (approximately 2×10^6 cells). Basal oxygen consumption rates were continuously measured on whole cells at 37°C, using a Clark-type oxygen electrode (Oroboros Oxygraph-2k, Oroboros Instruments, Innsbruck, Austria). For calibration of the polarographic oxygen sensor and measurement of background oxygen consumption, the medium without biological sample was added to the O2k-chamber. For each experimental condition, OCR was measured in the presence or absence of the F1F0-ATP synthase inhibitor – oligomycin (1 µM), the glycolysis inhibitor – 2-DG (5 mM), the protonophoric uncoupler – dinitrophenol (100 µM) and a mix of the mitochondrial complex III inhibitor – myxothiazol (1 µM) and the mitochondrial complex I inhibitor – rotenone (1 µM). Data were expressed as picomoles O_2 consumed by cells per second and per million of cells.

2.4. Cytotoxicity assay

A549^{Dual} were plated in 96-well plate with a density of seeding corresponding to 10,000 cells per well. Cells were then treated respectively with RPMI 2 g·L^{-1} glucose, supplemented (or not) with 2-mM L-glutamine, containing increasing doses of 2-DG (ranging from 1 mM to 20 mM). DMEM – DMSO 10% was used as a positive death inductor. 24 hours after, cells undergo for neutral red assay.

Cell viability was assessed with neutral red uptake assay, as described by Repetto et al. [31]. Briefly, after removal of the cell culture supernatant, 100 µL of medium containing 40 µg·mL^{-1} of neutral red was added to each well. Cells were then incubated during 2 hours at 37°C. Following incubation, medium was removed and cells were washed with PBS. Finally, 150 µL of neutral red destain (50% ethanol, 49% H2O, 1% glacial acetic acid) was added to each well. Absorbance was read at 540 nm using FLUOstar® Omega microplate reader (BMG LABTECH, Offenburg, Germany).

$$Cell\ viability\ (\%) = 100\ \times \frac{Experimental\ condition\ (OD_{540})}{Negative\ control\ (OD_{540})}$$

2.5. Cell stimulation or infection

151 Antiviral response was induced using polyriboinosinic:polyribocytidylic acid (poly:IC), a double stranded RNA
152 complexed with transfection reagents which improve its uptake. A549^{Dual} were cultured in RPMI-1640 (ref. P04-17550,
153 PAN Biotech, Aidenbach, Germany) supplemented with glucose (2 g·L^{-1}) and with or without L-glutamine upon
154 stimulation, to promote metabolic reprogramming. Briefly, cells were plated in RPMI-1640 supplemented with 10% FBS
155 containing 2 g·L^{-1} of glucose with L-glutamine at different concentrations (0 mM, 0.2 mM, 1 mM or 2mM). After 24
156 hours of adaptation, cells were stimulated during 6 hours using PIC at 0.25 µg·mL^{-1} to study early steps of IFN pathway
157 and 24 hours for late steps of IFN pathway (*e.g.*, ISGs production). In the same manner, assessment of antiviral
158 response following cellular respiration or glycolysis inhibition was achieved using 0.25 µg·mL^{-1} PIC and respectively 1
159 µg·mL^{-1} rotenone or 5 mM 2-DG during 24 hours on A549^{Dual} either cultured in RPMI-1640 with 2 g·L^{-1} glucose either
160 supplemented with L-glutamine 2 mM or not for 24 hours. Following stimulation, cell culture supernatant was
161 harvested and stored at -20°C, while cells were either used fresh in flow cytometry, fixed for immunofluorescence or
162 lysed using RLT Lysis Buffer (Qiagen, Hilden, Germany) for subsequent RNA extraction or using RIPA buffer for
163 subsequent protein preparation.
164 Cell infection was achieved on A549^{Dual}with Zika virus (ZIKV) and Dengue virus (DENV). Briefly, 24h after seeding,
165 medium was changed to RPMI-1640 either containing or not L-glutamine. After 24 hours of adaptation, cells were
166 infected for 24h in RPMI-1640 supplemented or not with L-glutamine with ZIKV and DENV at a multiplicity of infection
167 (MOI) of 2. Cells infected in conventional medium (*e.g.,* complete DMEM) were used as control of infection. Following
168 infection, total protein extract was harvested using RIPA buffer. Infection was monitored by detection of viral envelope
169 (E) protein using a panflaviviral anti-E antibody (4G2) in western blot. Cell culture supernatant was harvested for
170 luciferase activity assessment.
171 *2.6. RT-qPCR*
172 Total RNA has been extracted from cell lysates by using the RNeasy Plus Mini Kit (cat. 74136, Qiagen, Hilden,
173 Germany). The total cDNA was obtained by reverse transcription using random primers from Invitrogen (ref. 58875,
174 ThermoFisher, Waltham, MA, USA) and M-MLV reverse transcriptase enzyme (ref. M1708, Promega, Madison, WI, USA)
175 at 42 °C for 60 minutes. cDNA was then subjected to a quantitative polymerase chain reaction, using a CFX96 Connect™
176 Real Time Detection System (Bio-Rad, Hercule, CA, USA). For amplification, BlasTaq™ 2X qPCR MasterMix (ref. G892-1,
177 Applied Biological Materials, Vancouver, Canada) and specific primers were used to assess gene transcripts expression
178 for following targets: ISG56, ISG54, ISG15, ISG12, IRF1, Viperin, OAS1, CMPK2, lncRNA-NRIR, IFN-β, RNA polymerase II
179 and 18S ribosomal RNA. A threshold cycle (Ct) was calculated for each single sample amplification reaction in the
180 exponential phase of amplification, using Bio-Rad CFX Manager 3.1 (Bio-Rad, Hercule, CA, USA). Data obtained were
181 expressed as mean normalized expression, RNA polymerase II and 18S ribosomal RNA serving has housekeeping gene.
182 *2.7. Western blot*
183 Stimulated cells (see *2.4 Cell stimulation*) were lysed in 200 µL of radioimmunoprecipitation assay buffer (RIPA
184 buffer) at 4 ° C for 10 min. Lysate were sonicated at 0 °C for 1 min of pulse at 40% at 0.5 cycle using an Omni-Ruptor
185 4000 (Omni International, Dutscher, Issy-les-Moulineaux, France). Proteins from total cell extract were quantified using
186 BCA reagent according to manufacturer instructions (Sigma-Aldrich, Humeau, La Chapelle-Sur-Erdre, France). A
187 standardized amount of protein extracts was treated with Laemmli buffer containing 10 mM DTT and heated at 95 ° C
188 for 5 min. 15 µg of proteins were separated on precast NuPAGE gels 4 – 12% (Thermofischer, France) at 200V constant

189 for 35 minutes. Transfer was performed on NC Protan supported membrane with a 0.45 µm pores (Amersham, GE, Buc,
190 France) at 60 mA constant per gel for 2 hours using a semi-dry system. After transfer, the membranes were saturated
191 with 5% nonfat dry milk in PBS – Tween 0.1%. Membranes were then incubated successively with primary antibodies
192 and secondary antibodies diluted in PBS – Tween 0.1% – 1% nonfat dry milk. Blots were revealed with enhanced
193 chemiluminescence, ECL prime detection reagents (GE, Buc, France) using an Amersham Imager 680 (GE, Buc, France).

194 *2.8. Mitochondrial ROS measurement*

195 Mitochondrial ROS were measured with MitoSOX™ Red using a flow cytometry-based protocol [32]. Briefly,
196 $A549^{Dual}$ were washed with PBS 1X, harvested with trypsin / EDTA, and centrifuged at 800×*g* for 5 min. After three
197 washes, cells were resuspended in preheated RPMI 2 $g{\cdot}L^{-1}$ glucose without phenol red, supplemented or not with 2 mM
198 L-glutamine. MitoSOX™ Red at a final concentration of 5 µM was added to cell suspension and incubated for 30 min at
199 37°C. After three washes with preheated medium, the expression of MitoSOX™ is quantified in the PE channel by flow
200 cytometry, using a CytoFLEX (Beckman Coulter, CA, USA).

201 *2.9. Immunofluorescence*

202 $A549^{Dual}$ cells grown on glass coverslips were fixed with 3.7% paraformaldehyde – 50 mM HEPES – 150 mM NaCl at
203 room temperature for 10 min. Fixed cells were permeabilized with 0.1% Triton X-100 in PBS for 3 min. The coverslips
204 were incubated with primary antibodies in 1% BSA – PBS. Antigen – antibody binding was visualized with donkey anti-
205 mouse Alexa 488 Fluor-conjugated and donkey anti-rabbit Alexa 488 Fluor-conjugated secondary antibodies. Nucleus
206 morphology was revealed by 4',6-Diamidino-2-phenylindole dihydrochloride (DAPI) staining. The coverslips were
207 mounted with ibidi Mounting Medium (ref. 50001, ibidi, Gräfelfing, Germany) and fluorescence was observed using an
208 AXIO OBSERVER 7 equipped with the Apotome.2 (Zeiss, Oberkochen, Germany). The images were acquired with the
209 ZEN software version 3.1 (Zeiss, Oberkochen, Germany).

210 *2.10. Measurement of the IFN-β Pathway activation*

211 Activation of the Interferon regulatory factors (IRF) pathway was monitored by measuring Lucia luciferase activity
212 in $A549^{Dual}$ cells. It was evaluated using QUANTI-Luc substrate according to manufacturer's recommendations. Briefly,
213 100 µL of QUANTI-Luc substrate was added to 20 µL of cell culture supernatant and IRF-induced luciferase levels were
214 quantified by luminescence measurement using a Luminoskan™ microplate luminometer (ThermoFisher, Waltham, MA,
215 USA).

216 *2.11. Transcription factors prediction*

217 Prediction of potential binding sites for transcription factors in the promoter region of antiviral effectors was
218 achieved using PROMO tool from ALGGEN group, which based on TRANSFAC 8.3 [33,34]. Briefly, a sequence of at least
219 1000 bp upstream of the 1st exon of each of the following genes was recovered from the Ensembl database [35]: viperin
220 (ENSG00000134321), OAS1 (ENSG00000089127), ISG12 (ENSG00000165949), ISG15 (ENSG00000187608) and ISG54
221 (ENSG00000119922). These sequences were submitted to MultiSearchSites to search for binding sites that viperin and
222 OAS1 sequences share on the one hand and ISG12, ISG15, and ISG54 on the other, restricting the prediction to the
223 human set of transcription factors. A Venn diagram was then drawn to illustrate the transcription factors common or
224 specific to these groups [36].

225 *2.12. Statistical analyses*

226 For all figures except figures 1 and 2C, statistical analyses were performed by two-way ANOVA with Dunnett's
227 correction using Graph-Pad Prism software version 9. For figures 1 and 2C, statistical analyses were done using
228 unpaired T-test. Values of $p<0.05$ were considered statistically significant. The degrees of significance are indicated in
229 the figures captions as follow: *$p<0.0332$; ** $p<0.0021$; *** $p<0.0002$; **** $p<0.0001$.

230 **3. Results**

231 *3.1. Enhancement of OXPHOS occurs in presence of L-glutamine*

232 We have previously demonstrated the ability of cells to produce a more effective antiviral response if cellular
233 respiration was increased [22]. We then induced metabolic reprogramming of $A549^{Dual}$ cells by cultivating them in
234 galactose. Galactose was shown to anaplerotically feed TCA via L-glutamine production [29]. It is established in
235 literature that L-glutamine is both essential for antiviral response and viral progeny [28]. An open question in the
236 literature is whether this amino acid more beneficial to the infected host cell or to the virus, in this context. Also, It
237 remains to be established which mechanisms underlie these observations. In light of our previous results, we
238 hypothesized that L-glutamine would be essential for the establishment of an effective antiviral response, via the
239 supply of TCA and OXPHOS.

240 As a first step, we therefore evaluated the ability of L-glutamine to induce an increase in cellular respiration. To do
241 so, we cultured $A549^{Dual}$ cells in RPMI containing 2 $g \cdot L^{-1}$ glucose, supplemented or not with 2 mM L-glutamine. After 24h
242 of adaptation, we measured the O_2 consumption of $A549^{Dual}$ cells by oximetry, using different uncoupling agents. As
243 shown in **Figure 1A**, the two culture conditions lead to a different O_2 consumption rate. Indeed, the basal level of O_2
244 consumption is significantly increased in the presence of L-glutamine **(Figure 1B - left panel)**. Moreover, using 2,4-
245 dinitrophenol to force the passage of protons from the mitochondrial intermembrane space reveals that the maximal
246 respiratory capacity of $A549^{Dual}$ is also significantly increased – 40% higher – in the presence of L-glutamine **(Figure 1B –**
247 **middle panel)**. Finally, we measured the proportion of O_2 consumption not attributable to mitochondria, completely
248 uncoupling the mitochondrial respiratory chain using a mixture of rotenone and myxothiazol. Cells grown without L-
249 glutamine showed greater non-mitochondrial cellular respiration than cells grown in the presence of L-glutamine
250 **(Figure 1B - right panel)**. Notably, the proton leakage assessed through the use of oligomycin was not different
251 between the two culture conditions. Also, the use of 2-deoxyglucose (2-DG) induces a decrease in O_2 consumption but
252 with no significant difference between cells cultured with or without L-glutamine. Thus, we have shown that L-
253 glutamine induces an increase in cellular respiration in $A549^{Dual}$ which, according to our hypothesis, could be associated
254 with a greater antiviral response in an infectious context.

255 *3.2. The antiviral response is bivalent and varies according to metabolic context*

256 As mentioned above, the role of L-glutamine in infection is not well defined yet. Some believe that L-glutamine is
257 essential for virus progeny, making the virus addicted to L-glutamine [28]. Others suggest that L-glutamine is necessary
258 for the antiviral response, making the host cell addicted to L-glutamine during infection [37]. Assuming that L-glutamine
259 supports a metabolism based on OXPHOS, it seems reasonable to suppose that it would also support the development
260 of the antiviral response. In order to prove the host cell's addiction to L-glutamine for the development of the antiviral
261 response, we decided to use poly:IC (PIC) with increasing doses of L-glutamine. PIC is a dsRNA, widely used as pathogen
262 associated molecular pattern mimetic. Indeed, It is known to mimic replicating viral RNA and to trigger the antiviral

263 response, through activation of TLR3, RIG-I and RIG-I like receptors (RLR), resulting in type I IFNs production and ISGs
264 expression [38,39].

265 Thus, we cultured A549^{Dual} with increasing doses of L-glutamine (from 0 to 2 mM) for 24 h before stimulation with
266 PIC 0.25 µg·mL^{-1}. After 24h of stimulation, we assessed the development of the antiviral response by measuring ISGs
267 expression by RT-qPCR. All ISGs tested here (IRF1, ISG15, ISG56, ISG54 and ISG12) showed an increase in expression in
268 response to PIC. Also, interestingly, their expression increases in response to L-glutamine, consistently with the level of
269 expression found in cells cultured in complete DMEM. The difference in expression with cells cultured without L-
270 glutamine was significant as early as 0.2 mM L-glutamine, with levels varying between 2 and 5-fold more, depending on
271 the gene studied **(Figure 2A)**. To validate the effect observed at the transcriptional level, we assessed the synthesis of
272 proteins that rely on the ISRE promoter. Specifically, since we used A549^{Dual}, which expresses Lucia luciferase under the
273 control of an ISG54 minimal promoter along with five IFN-stimulated response elements (ISRE), we were able to
274 evaluate ISGs protein expression via luciferase secretion supernatant. Consequently, we examined the release of
275 luciferase into the supernatant of cells treated with PIC by measuring the emitted luminescence using the Lucia
276 luciferase substrate (QUANTI-Luc). Consistent with the results obtained from RT-qPCR, we detected a significant
277 increase in luciferase activity upon PIC stimulation and dose-dependently along with an increase in L-glutamine
278 concentration (up to 10-fold), representing a significant induction of antiviral proteins whose production is under the
279 control of ISRE **(Figure 2B)**.

280 OXPHOS within the mitochondria has been regularly associated with the production of mitochondrial reactive
281 oxygen species (mROS) that have several physiological functions [40]. Among the functions repeatedly associated with
282 these mROS is the promotion of the antiviral response [23,41]. Using MitoSOX™, we explored the formation of mROS in
283 our model by flow cytometry. Thus, after 6h of stimulation with PIC, the level of cells becoming positive for mROS was
284 greater in cells cultured with 2 mM L-glutamine, when compared to cells cultured without L-glutamine, illustrating the
285 transient production of mROS with the establishment of the early steps of the antiviral response (**Figure 2C and S1**).
286 Moreover, to confirm that antiviral response establishment is associated with increased mitochondrial activity and
287 OXPHOS, we repeated high resolution respirometry measurement after PIC stimulation (**Figure 2D**). As illustrated in
288 **Figure 2D and 2E,** PIC stimulation is linked to a higher OXPHOS in A549^{Dual} cultured in 2 mM L-glutamine versus cells
289 cultured without L-glutamine, whether basally or at maximum respiratory capacity, reinforcing the link between this
290 metabolic state and higher expression of antiviral effectors. These results were associated with increased TOM20
291 labeling in A549^{Dual} cells cultured in L-glutamine and treated with PIC for 6h (**Figure S2**). The increase in TOM20 signal is
292 another manifestation of a more functional mitochondrial network in the presence of L-glutamine, supporting OXPHOS
293 (**Figure 1, 2D and 2E**) and induction of mROS (**Figure 2C**).

294 Since a stimulation with PIC, as we have conducted, cannot summarize all aspects of infection, we endeavored to
295 deepen our work demonstrating that such a dependency on L-glutamine exists even during a viral infection. Thus, we
296 employed two RNA viruses from the *Flavivirus* family (Zika virus and Dengue virus) and were able to demonstrate that
297 during infection with these viruses (at MOI 2), the antiviral response is significantly affected by the presence of
298 glutamine in the cell culture medium.

299 As illustrated in the **Figure S3**, the antiviral response assessed here thanks to the A549^{Dual} reporter system, shows a
300 dose-dependently increase linked to the addition of glutamine, thus illustrating the dependency of this cellular
301 response on OXPHOS, even during viral infection.
302 Furthermore, to confirm that the increase in antiviral response is related to a specific effect of L-glutamine, cells
303 were stimulated with PIC 0.25 µg·mL^{-1} in the presence (or absence) of a solution of non-essential amino acids – NEAA
304 (0.1 mM L-alanine, 0.1 mM L-asparagine, 0.1 mM L-aspartic acid, 0.1 mM L-glutamic acid, 0.1 mM glycine, 0.1 mM L-
305 proline and 0.1 mM L-serine) to which 2 mM L-glutamine was added (or not). As shown in **Figure S4**, luciferase activity,
306 and therefore the antiviral response it reflects, was not increased in the presence of NEAA alone. Of note, the addition
307 of L-glutamine to this cocktail restored the previous results.
308 Surprisingly, the expression of some ISGs does not follow this trend, quite the contrary. Therefore, by evaluating
309 the expression of viperin and 2'-5'-oligoadenylate synthetase 1 (OAS1) by RT-qPCR under the same conditions, we
310 established that these genes are more highly expressed at low L-glutamine concentration. Indeed, their expression
311 decreases inversely (up to 7-fold) with increasing L-glutamine concentration **(Figure 3)**. This suggests that there is in fact
312 a dichotomy in the expression profile of ISGs depending on the predominant metabolic pathway at the time of PIC
313 stimulation. If OXPHOS is favored, through L-glutamine, there will be a greater expression of ISG12, ISG15, ISG54, ISG56
314 and IRF1. On the contrary, if glycolysis is promoted, in this case in the absence of L-glutamine, other ISGs will be
315 favored, such as OAS1 and viperin. To test the accuracy of this hypothesis, we needed to inhibit these different
316 metabolic pathways under infectious condition and evaluate the development of the antiviral response for the different
317 mentioned ISGs.
318 *3.3. Antiviral response is bivalent and relying alternatively on glycolysis or OXPHOS*
319 As before [22], we used rotenone at a concentration of 1 µg·mL^{-1} to inhibit OXPHOS. Since rotenone is a broad-
320 spectrum insecticide, piscicide and pesticide from vegetal origin, known to inhibit the complex I of mitochondrial
321 electron transport chain, thus blocking OXPHOS and associated production of ATP [42]. While 2-DG, at 5 mM was used
322 to inhibit glycolysis. Indeed, 2-DG is a glucose molecule with a 2-hydroxyl group replaced by hydrogen, leading to a
323 molecule unsuitable for glycolysis which competitively inhibits glucose-6-phosphate production by
324 phosphoglucoisomerase [43]. Of note, at the dose of 5 mM 2-DG exerts no cytotoxic effect, assessed by neutral red
325 uptake assay, on A549^{Dual} as shown in **Figure S5.** Thus, we used these inhibitors in combination with stimulation by 0.25
326 µg·mL^{-1} PIC, to study the impact of glycolysis and OXPHOS inhibition on the expression of the antiviral genes presented
327 above.
328 First, we assessed this expression at the gene level, using RT-qPCR. As before, expression of IRF1, ISG12, ISG15,
329 ISG54 and ISG56 was significantly increased following stimulation with PIC in the presence of 2 mM L-glutamine,
330 compared with cells cultured without L-glutamine **(Figure 4)**. On the contrary, viperin and OAS1 were expressed more
331 when cells were cultured without L-glutamine. The addition of 2-DG, and the subsequent inhibition of glycolysis,
332 resulted in no significant difference in the expression of IRF1, ISG12, ISG15 and ISG56. On the other hand, expression of
333 OAS1 and viperin is significantly altered in cells cultured without L-glutamine when glycolysis is inhibited **(Figure 4)**.
334 Therefore, we can conclude that, at the transcriptional level, the expression of genes such as OAS1 and viperin appears
335 to be dependent on glycolysis, whereas the expression of other genes (e.g., ISG12, ISG15, IRF1) is independent of this
336 metabolic pathway. Interestingly, the expression of these same genes is significantly inhibited in the presence of

337 rotenone when cells are cultured with L-glutamine. Their expression level even reached that of cells cultured without L-
338 glutamine, notably for ISG54 **(Figure 4)**. Regarding viperin, its expression appeared less sensitive to rotenone in cells
339 cultured without L-glutamine, illustrating that this gene is less dependent on OXPHOS than the others **(Figure 4)**. Thus,
340 we have demonstrated here that, at the transcriptional level, the increased expression of certain antiviral genes, such
341 as ISG54 and ISG15, in L-glutamine-cultured cells is related to the higher OXPHOS rate in these cells.

342 At the protein level, we again studied the luminescence emitted by secreted luciferase in response to PIC to
343 estimate the production of antiviral proteins under the control of the ISRE promoter. The results obtained are
344 consistent with those obtained at the gene level for IRF1, ISG12, ISG15, ISG54 and ISG56. Namely, a decrease in
345 luciferase activity, reflecting a reduction in the production of viral proteins under ISRE control, in response to rotenone
346 treatment **(Figure 5A)**. Finally, by Western blot, we found a higher signal for ISG56 and ISG15 in response to PIC for cells
347 cultured in L-glutamine compared to cells cultured without **(Figure 5B and S6)**. This signal decreased after rotenone
348 treatment, indicating that the up-regulated production of these antiviral proteins in L-glutamine-grown cells is indeed
349 related to higher OXPHOS. Viperin, also assessed by Western blot, follows an opposite pattern. Indeed, cells cultured
350 without L-glutamine show a higher signal in response to PIC, illustrating greater viperin production in these cells than in
351 cells cultured with L-glutamine. However, this production was reduced after inhibition of glycolysis by 2-DG **(Figure 5B**
352 **and S6)**.

353 *3.4. Viperin is expressed in a type I IFN-independent manner in glycolytic condition*

354 In an attempt to explain the specificity of viperin expression, we hypothesized that the viperin promoter region
355 could possibly contain an element enabling greater viperin expression in response to glycolysis. Therefore, we
356 evaluated the expression by RT-qPCR of cytidine / uridine monophosphate kinase 2 (CMPK2) and the lncRNA-negative
357 regulator of the IFN response (lncRNA-NRIR), both of which are expressed at the same time as viperin (**Figure 6A**)[44].
358 As shown in **Figure 6B**, expression of CMPK2 or lncRNA-NRIR did not vary between L-glutamine and L-glutamine-free
359 conditions. This result corroborates the fact that OAS1 also responds better in glycolysis, even though it does not
360 depend on the same promoter region as viperin.

361 We then attempted to determine whether the switch that leads to a dichotomy in the ISGs expression profile
362 between cells cultured in L-glutamine versus non-L-glutamine cells could be related to a difference in the expression of
363 type I IFNs between the two conditions. Thus, by RT-qPCR, we assessed IFN-β expression in response to a 6-hour
364 stimulation with PIC, in the presence or absence of L-glutamine. Interestingly, cells cultured without L-glutamine exert
365 an expression of IFN-β similar to that observed for cells cultured with 2 mM L-glutamine (**Figure 6C**). However, this
366 expression is not converted to the protein level, since the signal found for IFN-β is weaker for cells cultured without L-
367 glutamine, whether by Western Blot (**Figure 6D**) or immunofluorescence (**Figure 6E**). The higher expression of IFN-β in
368 cells cultured with 2 mM L-glutamine results in greater STAT2-mediated signaling in these cells compared to cells
369 cultured without L-glutamine, as evidenced by the stronger signal observed for pSTAT2 for this condition (**Figure 6D**).
370 Therefore, higher expression of ISGs such as ISG54, ISG15, or ISG56 would be associated with more efficient IFN-
371 dependent signaling in the presence of L-glutamine. On the other hand, the increase in viperin and OAS1 expression in
372 glycolysis appears to be independent of IFN signaling. At this point, we still assume that it is possible that the higher
373 expression of these two genes in response to PIC under glycolytic conditions may result from the activation of a
374 transcription factor specific to these two genes compared to the other genes studied here. We therefore sought

375 possible binding sites for transcription factors found in common between the viperin and OAS1 genes on the one hand,
376 and ISG15, ISG54 and ISG12 on the other. To do this, we analyzed a sequence of more than 1000 bp upstream of the
377 first exon of each of these genes, using PROMO tool, based on TRANSFAC 8.3. We then compared the reported binding
378 sites between these two analysis groups (**Figure 6F**). As shown in the Venn diagram, 58 potential binding sites are found
379 to be in common between viperin and OAS1, but only three of these sites are found to be specific to these genes
380 compared to the other ISGs tested: STAT5A, NF-Y, and E2F-1. Therefore, it is possible that one of these three
381 transcription factors is responsible for the expression of viperin and OAS1 in cells treated without L-glutamine.

382 **4. Discussion**

383 With the succession of viral epidemics, some of which have a global impact, research efforts to understand host
384 response mechanisms have intensified. While much progress has been made in understanding the role of metabolism
385 in the activation and function of immune cells, and therefore in understanding how these cells respond to viral
386 infection, depending on their metabolic setting, very little is known about the innate antiviral response of the infected
387 host cell. An interesting question is whether their metabolism influences the canonical antiviral response, namely the
388 IFN response.

389 It has been established on several occasions that, during viral infection, viruses manipulate host cell metabolism,
390 diverting them from OXPHOS to glycolysis [21]. This detour has been shown to be of particular interest in viral progeny,
391 as in the case of HIV and DENV [24,45,46]. However, the influence of such hijacking on the production of antiviral
392 effector molecules induced by the IFN response has not yet been explored. The role of glutaminergic metabolism in the
393 antiviral response also remains unresolved in the literature: does the benefit fall to the virus or to the host cell in the
394 event of infection [28]? We have previously shown that OXPHOS promotes the expression of certain antiviral effectors
395 such as ISG54 and ISG56. Furthermore, given that glutaminergic metabolism is closely linked to OXPHOS through
396 anaplerotic feeding of TCA, we hypothesized here that glutamine intake in an infectious context would increase the
397 antiviral response and the production of antiviral effectors. To address this hypothesis, we stimulated A549^{Dual} cells
398 with PIC in the presence or absence of L-glutamine, in order to study the intrinsic effect of metabolism on the antiviral
399 response, while avoiding the inhibitory effect that viral proteins can induce during infection.

400 Here, we were able to demonstrate that cells cultured with 2 mM L-glutamine had more functional mitochondria
401 (**Figure 1 and S2**), which supported greater induction of OXPHOS and mROS (**Figures 1, 2C and 2D**). Furthermore, the
402 increased mitochondrial activity in these cells was correlated with a greater production of certain antiviral effectors
403 (ISG12, ISG15, ISG54, ISG56, IRF1), as shown by inhibition of their expression in the presence of rotenone (**Figures 2, 4**
404 **and 5**). Moreover, this increased antiviral state in presence of glutamine was observed during viral infection using ZIKV
405 and DENV (**Figure S3**). However, we were also able to show that the expression of certain ISGs escapes the need for
406 OXPHOS, since viperin and OAS1 are more highly expressed in the presence of aerobic glycolysis (**Figures 3, 4 and 5**).
407 One factor that may explain this dichotomy is that IFN-β expression and subsequent signaling are greater in cells to
408 which L-glutamine has been added (**Figure 6**). While higher expression of viperin and OAS1 could be related to a specific
409 transcription factor such as E2F-1 (**Figure 6F**).

410 It had previously been shown that viperin expression was increased under conditions of high glucose and therefore
411 glycolysis, enabling control of Zika virus infection [47]. These results were surprising in light of our work illustrating the
412 beneficial effect of OXPHOS on the production of other antiviral effectors such as ISG54 and ISG56 [22]. Our study

413 reconciles these results, as we have demonstrated the existence of a bivalent antiviral response, the orientation of
414 which depends on cellular metabolic status (**Figure 7**). Therefore, OXPHOS in L-glutamine culture favors the production
415 of ISGs such as ISG12, 15, 54 and 56. Whereas, glycolysis is beneficial for the production of viperin and OAS1. These
416 results suggest that the bivalence of the antiviral response may be of interest in the event of metabolic reprogramming
417 by the virus, with one taking over from the other. Thus, in the case of a Warburg-like effect, the host cell can still base
418 its antiviral response on the induction of potent antiviral effectors such as viperin or OAS1. Furthermore, our results
419 showed that the promotion of OXPHOS by glutamine favored the antiviral response, even in a context of total infection,
420 using Dengue and Zika viruses. The results we obtained are consistent with what is already known for these viruses.
421 During infection, DENV and ZIKV showed an early capacity to divert cellular metabolism towards glycolysis. Thus, 10
422 h.p.i. an increase in lactate produced by DENV-infected cells was reported [45,48]. In addition, a significant decrease in
423 OXPHOS was demonstrated 24 h.p.i. in infected HUH7 [49]. Similar results were obtained for ZIKV, with a 12 h.p.i.
424 decrease in OXPHOS [50]. The diversion of cellular metabolism towards glycolysis clearly favors the virus during the
425 early phases of its viral cycle, on the one hand by enabling the production of biomass through a Warburg-like effect, but
426 also, as we have been able to demonstrate with our results, by limiting the development of the antiviral response.
427 However, as demonstrated in the literature, this process of diversion cannot last throughout the infection. Indeed, later
428 energy-intensive processes, such as the transition through the secretory pathway, may require the production of large
429 amount of energy, which explains the reduction in OXPHOS observed at 48 h.p.i. [51]. Control of antiviral response due
430 to OXPHOS in this phase of infection would therefore be done by regulation of endoplasmic reticulum-mitochondria
431 interfaces as demonstrated by the ability of DENV NS4B to regulate mitochondrial fission by inhibition of DRP1, leading
432 to mitochondria-associated membranes disruption and thus, subsequent inhibition of RIG-I dependent antiviral
433 response [25]. The regulation of cellular metabolism by these viruses during infection therefore seems to be associated
434 with precise mechanisms, the sequence of which is always designed to promote viral replication and progeny.
435 Promoting OXPHOS and the antiviral response that may be associated with it could therefore be beneficial in limiting
436 viral replication. However, the question of glutamine dependence may arise and seems to affect ZIKV and DENV rather
437 than the host, since these viruses do not seem to be able to replicate in the absence of glutamine (as shown in **Figure**
438 **S3**). In this case, should we favor the OXPHOS-dependent antiviral response (ISG15, 56 and 54)? Or should we limit
439 glutamine intake, which would inhibit viral replication while allowing expression of glycolysis-dependent ISGs (viperin
440 and OAS1)? Of note, it should be mentioned that the study of the influence of viral infection on metabolism is complex.
441 The data currently available in the literature illustrate a variation in the effect of viral infection on metabolism
442 depending on the infected host. This is particularly true for the Zika virus, which behaves differently it infects its vector,
443 the mosquito [52].

444 However, through this work we have not been able to uncover the mechanism leading to greater expression of
445 viperin in a glycolytic context. And this important aspect remains to be explored in future work. We hypothesize that
446 the expression of viperin and OAS1 could be linked to the activation of a specific transcription factor in this context.
447 Among those we have identified (**Figure 6F**), it is known that E2F-1 is normally sequestered by retinoblastoma protein
448 (Rb). In the presence of glucose, E2F-1/pRB axis is more active, leading to release of E2F-1 and transcription of its
449 targets . However, everything may not be solely linked to this transcription factor, and we cannot rule out that it may
450 be a combination of various factors or even a specific timing that promotes the expression of viperin and OAS1 duing

aerobic glycolysis. Additionally, it is possible to argue that viperin is known to be expressed independently of interferon in a mode involving NF-κB. These hypotheses should be explored in future studies. Finally, we have been able to demonstrate that OXPHOS promotes IFN-β production, in contrast to glycolysis, leading to a more efficient production of antiviral effectors.

In the light of our initial results, it might be possible to argue that the glutamine addiction discussed in the literature initially seems to go to the host cell, since it produces more antiviral effectors in the presence of L-glutamine. However, since some antiviral effectors can overcome this dependence, it seems that glutamine is more essential to the virus for its progeny [28]. This suggests an adaptive mechanism whereby, to counteract the virus-induced metabolic reprogramming that undermines the antiviral response carried out by ISGs (12, 15, 54 and 56), the host cell has found a way to promote the production of other effectors such as viperin and OAS1. We could be in a frenetic adaptive race in which the cellular metabolic status is of prime importance. These results are encouraging and suggest that the study of glutaminergic metabolism could be an interesting way of approaching the control of a viral infection, and thus exploring possible therapeutic or preventive opportunities. However, these data still need to be consolidated and further experiments on animal model should be considered to confirm these mechanisms *in vivo*. There is some evidence to suggest that OXPHOS in vivo is favorable, since the pattern presented here is reminiscent of the antiviral response in bats. Indeed, these mammals are the only ones to have acquired the ability to fly, which is associated with a high respiratory capacity and, consequently, high ROS production. This favors the interferon response in these mammals and confers on them the ability to control most of the pathogens that infect them, limiting the associated pathophysiology [53–55].

Author Contributions

Investigation, resources, data curation, G.L., M.H., A.P.R., D.E.S, P.K.-T. and W.V.; writing—original draft preparation, G.L.; writing—review and editing, G.L., M.H., D.E.S, A.P.R., O.M., P.K.-T., M.R. and W.V.; Methodology, G.L. and W.V.; formal analysis, G.L. and W.V.; supervision, W.V.; Conceptualization, G.L., O.M., and W.V.; funding acquisition, G.L., M.R. and W.V.; All authors have read and agreed to the published version of the manuscript.

Acknowledgments

We would like to thank all our colleagues from PIMIT and DéTROI and especially the Dr. Pascal Baret for his thankful help during this work. Graphical abstract was created using Biorender.com.

Funding

This research was funded by the CASI project (supported by BioST federation of Université de La Réunion). G.L., D.E.S and A.P.R. have PhD degree scholarship from Réunion University (Ecole doctorale STS) funded by DIRED/2021-0161, DIRED/2021-1115 and DIRED/2021-1124 from Région Réunion, respectively. We want to acknowledge the Dr. Philippe Desprès for his thoughtful advices.

Informed Consent Statement

Not applicable.

Data Availability Statement

All data needed to evaluate the conclusions in the paper are present in the article and/or the Supplementary Materials. Additional data related to this paper are available from the corresponding author upon reasonable request.

Conflicts of Interest

The authors declare no conflict of interest.

References

[1] Ksiazek TG, Erdman D, Goldsmith CS, Zaki SR, Peret T, Emery S, et al. A Novel Coronavirus Associated with Severe Acute Respiratory Syndrome. N Engl J Med 2003;348:1953–66. https://doi.org/10.1056/NEJMoa030781.

[2] Novel Swine-Origin Influenza A (H1N1) Virus Investigation Team, Dawood FS, Jain S, Finelli L, Shaw MW, Lindstrom S, et al. Emergence of a novel swine-origin influenza A (H1N1) virus in humans. N Engl J Med 2009;360:2605–15. https://doi.org/10.1056/NEJMoa0903810.

[3] Zaki AM, van Boheemen S, Bestebroer TM, Osterhaus ADME, Fouchier RAM. Isolation of a Novel Coronavirus from a Man with Pneumonia in Saudi Arabia. N Engl J Med 2012;367:1814–20. https://doi.org/10.1056/NEJMoa1211721.

[4] Baize S, Pannetier D, Oestereich L, Rieger T, Koivogui L, Magassouba N, et al. Emergence of Zaire Ebola Virus Disease in Guinea. New England Journal of Medicine 2014;371:1418–25. https://doi.org/10.1056/NEJMoa1404505.

[5] Faria NR, Azevedo R do S da S, Kraemer MUG, Souza R, Cunha MS, Hill SC, et al. Zika virus in the Americas: Early epidemiological and genetic findings. Science 2016;352:345–9. https://doi.org/10.1126/science.aaf5036.

[6] Zhou P, Yang X-L, Wang X-G, Hu B, Zhang L, Zhang W, et al. A pneumonia outbreak associated with a new coronavirus of probable bat origin. Nature 2020;579:270–3. https://doi.org/10.1038/s41586-020-2012-7.

[7] Thornhill JP, Barkati S, Walmsley S, Rockstroh J, Antinori A, Harrison LB, et al. Monkeypox Virus Infection in Humans across 16 Countries — April–June 2022. New England Journal of Medicine 2022;0:null. https://doi.org/10.1056/NEJMoa2207323.

[8] Majzoub K, Wrensch F, Baumert TF. The Innate Antiviral Response in Animals: An Evolutionary Perspective from Flagellates to Humans. Viruses 2019;11:758. https://doi.org/10.3390/v11080758.

[9] Chow KT, Gale M, Loo Y-M. RIG-I and Other RNA Sensors in Antiviral Immunity. Annu Rev Immunol 2018;36:667–94. https://doi.org/10.1146/annurev-immunol-042617-053309.

[10] Motwani M, Pesiridis S, Fitzgerald KA. DNA sensing by the cGAS–STING pathway in health and disease. Nat Rev Genet 2019;20:657–74. https://doi.org/10.1038/s41576-019-0151-1.

[11] Schoggins JW. Interferon-Stimulated Genes: What Do They All Do? Annu Rev Virol 2019;6:567–84. https://doi.org/10.1146/annurev-virology-092818-015756.

[12] Schneider WM, Chevillotte MD, Rice CM. Interferon-Stimulated Genes: A Complex Web of Host Defenses. Annu Rev Immunol 2014;32:513–45. https://doi.org/10.1146/annurev-immunol-032713-120231.

[13] Dixit E, Boulant S, Zhang Y, Lee ASY, Odendall C, Shum B, et al. Peroxisomes Are Signaling Platforms for Antiviral Innate Immunity. Cell 2010;141:668–81. https://doi.org/10.1016/j.cell.2010.04.018.

[14] Odendall C, Dixit E, Stavru F, Bierne H, Franz KM, Durbin AF, et al. Diverse intracellular pathogens activate type III interferon expression from peroxisomes. Nat Immunol 2014;15:717–26. https://doi.org/10.1038/ni.2915.

[15] Schoggins JW, Rice CM. Interferon-stimulated genes and their antiviral effector functions. Current Opinion in Virology 2011;1:519–25. https://doi.org/10.1016/j.coviro.2011.10.008.

[16] McNab F, Mayer-Barber K, Sher A, Wack A, O'Garra A. Type I interferons in infectious disease. Nat Rev Immunol 2015;15:87–103. https://doi.org/10.1038/nri3787.

[17] Beyer DK, Forero A. Mechanisms of Antiviral Immune Evasion of SARS-CoV-2. Journal of Molecular Biology 2022;434:167265. https://doi.org/10.1016/j.jmb.2021.167265.

[18] Meylan E, Curran J, Hofmann K, Moradpour D, Binder M, Bartenschlager R, et al. Cardif is an adaptor protein in the RIG-I antiviral pathway and is targeted by hepatitis C virus. Nature 2005;437:1167–72. https://doi.org/10.1038/nature04193.

[19] Mesev EV, LeDesma RA, Ploss A. Decoding type I and III interferon signalling during viral infection. Nat Microbiol 2019;4:914–24. https://doi.org/10.1038/s41564-019-0421-x.

[20] Loftus RM, Finlay DK. Immunometabolism: Cellular Metabolism Turns Immune Regulator. Journal of Biological Chemistry 2016;291:1–10. https://doi.org/10.1074/jbc.R115.693903.

[21] Thaker SK, Ch'ng J, Christofk HR. Viral hijacking of cellular metabolism. BMC Biology 2019;17:59. https://doi.org/10.1186/s12915-019-0678-9.

[22] Lebeau G, El Safadi D, Paulo-Ramos A, Hoareau M, Desprès P, Krejbich-Trotot P, et al. The Efficient Antiviral Response of A549 Cells Is Enhanced When Mitochondrial Respiration Is Promoted. Pathogens 2022;11:1168. https://doi.org/10.3390/pathogens11101168.

[23] Buskiewicz IA, Montgomery T, Yasewicz EC, Huber SA, Murphy MP, Hartley RC, et al. Reactive oxygen species induce virus-independent MAVS oligomerization in systemic lupus erythematosus. Sci Signal 2016;9. https://doi.org/10.1126/scisignal.aaf1933.

[24] Angin M, Volant S, Passaes C, Lecuroux C, Monceaux V, Dillies M-A, et al. Metabolic plasticity of HIV-specific CD8 + T cells is associated with enhanced antiviral potential and natural control of HIV-1 infection. Nature Metabolism 2019;1:704–16. https://doi.org/10.1038/s42255-019-0081-4.

[25] Chatel-Chaix L, Cortese M, Romero-Brey I, Bender S, Neufeldt CJ, Fischl W, et al. Dengue Virus Perturbs Mitochondrial Morphodynamics to Dampen Innate Immune Responses. Cell Host & Microbe 2016;20:342–56. https://doi.org/10.1016/j.chom.2016.07.008.

[26] Carneiro L, Guissard C, Offer G, Belenguer P, Pénicaud L, Leloup C. The mitochondrial fission induced by glucose is essential to the ROS signaling in hypothalamic detection of hyperglycemia. Diabetes & Metabolism 2010;36:A38. https://doi.org/10.1016/S1262-3636(10)70145-2.

[27] Zhang W, Wang G, Xu Z-G, Tu H, Hu F, Dai J, et al. Lactate Is a Natural Suppressor of RLR Signaling by Targeting MAVS. Cell 2019;178:176-189.e15. https://doi.org/10.1016/j.cell.2019.05.003.

[28] Koufaris C, Nicolaidou V. Glutamine addiction in virus-infected mammalian cells: A target of the innate immune system? Med Hypotheses 2021;153:110620. https://doi.org/10.1016/j.mehy.2021.110620.
[29] Shiratori R, Furuichi K, Yamaguchi M, Miyazaki N, Aoki H, Chibana H, et al. Glycolytic suppression dramatically changes the intracellular metabolic profile of multiple cancer cell lines in a mitochondrial metabolism-dependent manner. Sci Rep 2019;9:18699. https://doi.org/10.1038/s41598-019-55296-3.
[30] Frumence E, Roche M, Krejbich-Trotot P, El-Kalamouni C, Nativel B, Rondeau P, et al. The South Pacific epidemic strain of Zika virus replicates efficiently in human epithelial A549 cells leading to IFN-β production and apoptosis induction. Virology 2016;493:217–26. https://doi.org/10.1016/j.virol.2016.03.006.
[31] Repetto G, del Peso A, Zurita JL. Neutral red uptake assay for the estimation of cell viability/cytotoxicity. Nat Protoc 2008;3:1125–31. https://doi.org/10.1038/nprot.2008.75.
[32] Yang Y, Zhang G, Yang T, Gan J, Xu L, Yang H. A flow-cytometry-based protocol for detection of mitochondrial ROS production under hypoxia. STAR Protocols 2021;2:100466. https://doi.org/10.1016/j.xpro.2021.100466.
[33] Messeguer X, Escudero R, Farré D, Núñez O, Martínez J, Albà MM. PROMO: detection of known transcription regulatory elements using species-tailored searches. Bioinformatics 2002;18:333–4. https://doi.org/10.1093/bioinformatics/18.2.333.
[34] Farré D, Roset R, Huerta M, Adsuara JE, Roselló L, Albà MM, et al. Identification of patterns in biological sequences at the ALGGEN server: PROMO and MALGEN. Nucleic Acids Research 2003;31:3651–3. https://doi.org/10.1093/nar/gkg605.
[35] Martin FJ, Amode MR, Aneja A, Austine-Orimoloye O, Azov AG, Barnes I, et al. Ensembl 2023. Nucleic Acids Research 2023;51:D933–41. https://doi.org/10.1093/nar/gkac958.
[36] Heberle H, Meirelles GV, Da Silva FR, Telles GP, Minghim R. InteractiVenn: a web-based tool for the analysis of sets through Venn diagrams. BMC Bioinformatics 2015;16:169. https://doi.org/10.1186/s12859-015-0611-3.
[37] Wang K, Hoshino Y, Dowdell K, Bosch-Marce M, Myers TG, Sarmiento M, et al. Glutamine supplementation suppresses herpes simplex virus reactivation. Journal of Clinical Investigation 2017;127:2626–30. https://doi.org/10.1172/JCI88990.
[38] Gitlin L, Barchet W, Gilfillan S, Cella M, Beutler B, Flavell RA, et al. Essential role of mda-5 in type I IFN responses to polyriboinosinic:polyribocytidylic acid and encephalomyocarditis picornavirus. Proc Natl Acad Sci U S A 2006;103:8459–64. https://doi.org/10.1073/pnas.0603082103.
[39] Kato H, Sato S, Yoneyama M, Yamamoto M, Uematsu S, Matsui K, et al. Cell type-specific involvement of RIG-I in antiviral response. Immunity 2005;23:19–28. https://doi.org/10.1016/j.immuni.2005.04.010.
[40] Zorov DB, Juhaszova M, Sollott SJ. Mitochondrial Reactive Oxygen Species (ROS) and ROS-Induced ROS Release. Physiological Reviews 2014;94:909–50. https://doi.org/10.1152/physrev.00026.2013.
[41] Nobre L, Wise D, Ron D, Volmer R. Modulation of Innate Immune Signalling by Lipid-Mediated MAVS Transmembrane Domain Oligomerization. PLoS ONE 2015;10:e0136883. https://doi.org/10.1371/journal.pone.0136883.
[42] Heinz S, Freyberger A, Lawrenz B, Schladt L, Schmuck G, Ellinger-Ziegelbauer H. Mechanistic Investigations of the Mitochondrial Complex I Inhibitor Rotenone in the Context of Pharmacological and Safety Evaluation. Sci Rep 2017;7:45465. https://doi.org/10.1038/srep45465.
[43] Wick AN, Drury DR, Nakada HI, Wolfe JB. Localization of the primary metabolic block produced by 2-deoxyglucose. J Biol Chem 1957;224:963–9.
[44] Kambara H, Niazi F, Kostadinova L, Moonka DK, Siegel CT, Post AB, et al. Negative regulation of the interferon response by an interferon-induced long non-coding RNA. Nucleic Acids Research 2014;42:10668–80. https://doi.org/10.1093/nar/gku713.
[45] Fontaine KA, Sanchez EL, Camarda R, Lagunoff M. Dengue Virus Induces and Requires Glycolysis for Optimal Replication. Journal of Virology 2015;89:2358–66. https://doi.org/10.1128/JVI.02309-14.
[46] Valle-Casuso JC, Angin M, Volant S, Passaes C, Monceaux V, Mikhailova A, et al. Cellular Metabolism Is a Major Determinant of HIV-1 Reservoir Seeding in CD4+ T Cells and Offers an Opportunity to Tackle Infection. Cell Metabolism 2019;29:611-626.e5. https://doi.org/10.1016/j.cmet.2018.11.015.
[47] Reslan A, Haddad JG, Desprès P, Bascands J-L, Gadea G. High Glucose Induces in HK2 Kidney Cells an IFN–Dependent ZIKV Antiviral Status Fueled by Viperin. Biomedicines 2022;10:1577. https://doi.org/10.3390/biomedicines10071577.
[48] Allonso D, Andrade IS, Conde JN, Coelho DR, Rocha DCP, Da Silva ML, et al. Dengue Virus NS1 Protein Modulates Cellular Energy Metabolism by Increasing Glyceraldehyde-3-Phosphate Dehydrogenase Activity. J Virol 2015;89:11871–83. https://doi.org/10.1128/JVI.01342-15.
[49] Fernandes-Siqueira LO, Zeidler JD, Sousa BG, Ferreira T, Da Poian AT. Anaplerotic Role of Glucose in the Oxidation of Endogenous Fatty Acids during Dengue Virus Infection. mSphere 2018;3:e00458-17. https://doi.org/10.1128/mSphere.00458-17.
[50] Chen Q, Gouilly J, Ferrat YJ, Espino A, Glaziou Q, Cartron G, et al. Metabolic reprogramming by Zika virus provokes inflammation in human placenta. Nat Commun 2020;11:2967. https://doi.org/10.1038/s41467-020-16754-z.
[51] Barbier V, Lang D, Valois S, Rothman AL, Medin CL. Dengue virus induces mitochondrial elongation through impairment of Drp1-triggered mitochondrial fission. Virology 2017;500:149–60. https://doi.org/10.1016/j.virol.2016.10.022.
[52] Thaker SK, Chapa T, Garcia G, Gong D, Schmid EW, Arumugaswami V, et al. Differential Metabolic Reprogramming by Zika Virus Promotes Cell Death in Human versus Mosquito Cells. Cell Metabolism 2019;29:1206-1216.e4. https://doi.org/10.1016/j.cmet.2019.01.024.
[53] Brook CE, Dobson AP. Bats as 'special' reservoirs for emerging zoonotic pathogens. Trends in Microbiology 2015;23:172–80. https://doi.org/10.1016/j.tim.2014.12.004.
[54] Zhou P, Tachedjian M, Wynne JW, Boyd V, Cui J, Smith I, et al. Contraction of the type I IFN locus and unusual constitutive expression of *IFN-α* in bats. Proc Natl Acad Sci USA 2016;113:2696–701. https://doi.org/10.1073/pnas.1518240113.

[55] Kacprzyk J, Hughes GM, Palsson-McDermott EM, Quinn SR, Puechmaille SJ, O'Neill LAJ, et al. A Potent Anti-Inflammatory Response in Bat Macrophages May Be Linked to Extended Longevity and Viral Tolerance. Acta Chiropterologica 2017;19:219–28. https://doi.org/10.3161/15081109ACC2017.19.2.001.

Figures caption

Figure 1 – OXPHOS is associated with L-glutamine-containing medium. (A) Comparison of the oxygen consumption rate of A549^{Dual} cultured with or without L-glutamine. 5 mM 2-deoxyglucose (2-DG) has been used to inhibit hexokinase activity and glycolysis. 1 µM oligomycin (Oligo) has been used to inhibit ATP synthase. 100 µM 2,4-dinitrophenol (DNP) has been used as protonophoric uncoupler, allowing maximal respiration. 1 µM Rotenone – 1 µM Myxothiazol has been used to uncouple both mitochondrial complex I and III, illustrating non mitochondrial respiration. The metabolism of cells grown in RPMI supplemented with 2 mM L-glutamine is more dependent on oxidative phosphorylation. (B) More specifically, cells cultured with L-glutamine have higher basal O_2 consumption flux, associated with higher maximal respiration capacity and consistently lower non mitochondrial respiration. Error bars represent standard deviation of three independent experiments. *p<0.0332; **** p<0.000

Figure 2 – L-glutamine increases antiviral response to poly:IC. (A) L-glutamine related overexpression of ISGs expression. The expression of several ISGs (IRF1, ISG15, ISG56, ISG54, ISG12) has been assessed by RT-qPCR after 24-hour stimulation of A549^{Dual}, grown in RPMI 2 g·L^{-1} glucose, supplemented with increasing doses of L-glutamine (0, 0.2, 1 and 2 mM), using PIC 0.25 µg·mL^{-1}. Results are expressed as mean normalized expression, following normalization with expression of 18S ribosomal RNA as a housekeeping gene. (B) ISRE-dependent proteins increased production in presence of L-glutamine. Evaluation of IRF pathway activation in response to PIC 0.25 µg·mL^{-1} stimulation of A549^{Dual} grown in RPMI 2 g·L^{-1} glucose supplemented with increasing doses of L-glutamine (0, 0.2, 1 and 2 mM) was achieved by measuring activity of secreted Lucia luciferase, using QUANTI-Luc substrate 24 hours after treatment. Results are expressed as emitted luminescence intensity. (C) mROS induction is higher in presence of L-glutamine. Mitochondrial ROS were measured with MitoSOX™ Red using a flow cytometry-based protocol in cells grown in RPMI 2 g·L^{-1} glucose, supplemented or not with 2 mM L-glutamine, after 6h of stimulation with PIC. Error bars represent standard deviation of three independent experiments. *p<0.0332; ** p<0.0021; *** p<0.0002; **** p<0.0001. (D) Comparison of the oxygen consumption rate of A549^{Dual} cultured with or without L-glutamine and stimulated with poly:IC. 5 mM 2-deoxyglucose (2-DG) has been used to inhibit hexokinase activity and glycolysis. 1 µM oligomycin (Oligo) has been used to inhibit ATP synthase. 100 µM 2,4-dinitrophenol (DNP) has been used as protonophoric uncoupler, allowing maximal respiration. 1 µM Rotenone – 1 µM Myxothiazol has been used to uncouple both mitochondrial complex I and III, illustrating non mitochondrial respiration. Poly:IC stimulation induces a higher rate of OXPHOS in cells grown in RPMI supplemented with L-glutamine than cells cultured without L-glutamine. (E) More specifically, cells cultured with L-glutamine have higher basal O_2 consumption flux, associated with higher maximal respiration capacity and consistently lower non mitochondrial respiration, in response to poly:IC stimulation. Error bars represent standard deviation of three independent experiments. **** p<0.0001.

Figure 3 – Expression of OAS1 and viperin are independent L-glutamine. Expression of OAS1 and viperin was assessed by RT-qPCR following a 24-hour stimulation of A549^{Dual}, grown in RPMI 2 g·L^{-1} glucose, supplemented with increasing doses of L-glutamine (0, 0.2, 1 and 2 mM), using PIC 0.25 µg·mL^{-1}. Results are expressed as mean normalized expression, following normalization with expression of 18S ribosomal RNA as a housekeeping gene. Error bars represent standard deviation of three independent experiments. *** p<0.0002; **** p<0.0001.

Figure 4 – Bivalent expression of ISGs is based on glycolysis and OXPHOS. Expression of several ISGs (IRF1, ISG15, ISG56, ISG54, ISG12, OAS1 and viperin) have been assessed by RT-qPCR following a 24-hour stimulation of A549^{Dual}, grown in RPMI 2 g·L^{-1} glucose, supplemented or not with 2 mM L-glutamine, using PIC 0.25 µg·mL^{-1}. Simultaneously, to evaluate the influence of glycolysis and OXPHOS on the upregulation of ISGs regarding L-glutamine supplementation, 5 mM 2-deoxyglucose (2-DG) and 1 µg·mL^{-1} rotenone were used to inhibit glycolysis and OXPHOS respectively. Results are expressed as mean normalized expression, following normalization with expression of RNA polymerase II RNA as a housekeeping gene. The error bars represent standard deviation of three independent experiments. *p<0.0332; ** p<0.0021; *** p<0.0002; **** p<0.0001 as compared to PIC. $^{\$}$ p<0.0332; $^{\$\$}$ p<0.0021; $^{\$\$\$}$ p<0.0002; $^{\$\$\$\$}$ p<0.0001 comparison between without L-glutamine vs. with L-glutamine.

Figure 5 – Bivalent ISG production depends on glycolysis or OXPHOS. (A) ISRE-dependent proteins increased production in presence of L-glutamine is linked to OXPHOS. Evaluation of IRF pathway activation in response to

PIC 0.25 µg·mL^{-1} stimulation of A549^{Dual} grown in RPMI 2 g·L^{-1} glucose, supplemented or not with 2 mM L-glutamine, was achieved by measuring activity of secreted Lucia luciferase, using QUANTI-Luc substrate 24 hours after treatment. Concomitantly, to assess the influence of glycolysis and OXPHOS on the upregulation of ISGs with respect to L-glutamine supplementation, 5 mM 2-deoxyglucose (2-DG) and 1 µg·mL^{-1} rotenone were used to inhibit glycolysis and OXPHOS. Results are expressed as fold change in emitted luminescence intensity from mock stimulated cells. Error bars represent standard deviation from three independent experiments. ** $p<0.0021$; *** $p<0.0002$. (B) Bivalent production of ISGs relies on either glycolysis or OXPHOS. ISGs production in response to PIC 0.25 µg·mL^{-1} stimulation of A549^{Dual} grown in RPMI 2 g·L^{-1} glucose, supplemented or not with 2 mM L-glutamine, was achieved by western blot analysis. Western blot assay was achieved with mouse anti-ISG56, rabbit anti-ISG15, mouse anti-viperin and rabbit anti-β-tubulin antibodies. These images are representative of three independent experiments. Bands density was evaluated and signal emission normalized to protein loading. Error bars represent standard deviation from three independent experiments. * $p<0.0332$; ** $p<0.0021$; *** $p<0.0002$; **** $p<0.0001$.

Figure 6 – Differential expression of ISGs correlates with variable IFN-β signaling. (A) Schematic representation of viperin, CMPK2 and lc-NRIR loci on chromosome 2. Exon/intron structure of genes is represented, promoter region is annotated and arrows indicate the orientation of transcription for each locus. (B) CMPK2 and lc-NRIR are expressed in the same manner under glycolytic and OXPHOS conditions. The expression of CMPK2 and lc-NRIR has been assessed by RT-qPCR after 24-hour stimulation of A549^{Dual}, grown in RPMI 2 g·L^{-1} glucose, supplemented or not 2 mM L-glutamine, using PIC 0.25 µg·mL^{-1}. Results are expressed as mean normalized expression, following normalization with expression of RNA polymerase II RNA as a housekeeping gene. (C) IFN-β mRNA has the same level of expression under glycolytic and OXPHOS conditions. The expression of IFN-β has been assessed by RT-qPCR after 6-hour stimulation of A549^{Dual}, grown in RPMI 2 g·L^{-1} glucose, supplemented or not with 2 mM L-glutamine, using PIC 0.25 µg·mL^{-1}. Results are expressed as mean normalized expression, following normalization with expression of RNA polymerase II RNA as a housekeeping gene. Error bars represent standard deviation from three independent experiments. * $p<0.0332$; ** $p<0.0021$. (D, E) Alternative ISGs expression is related to IFN-β production and signaling. IFN-β production and phosphorylation of STAT2 in response to PIC stimulation of A549^{Dual} grown in RPMI 2 g·L^{-1} glucose, supplemented or not with 2 mM L-glutamine, was achieved by western blot analysis and immunofluorescence. Western blot assay was achieved with mouse anti-IFN-β, rabbit anti-pSTAT2, and rabbit anti-β-tubulin antibodies. Immunofluorescence assay was achieved using mouse anti-IFN-β, donkey anti-mouse Alexa 488 and DAPI. These images are representative of three independent experiments. Error bars represent standard deviation from three independent experiments. * $p<0.0332$; **** $p<0.0001$. (F) Overexpression of viperin and OAS1 could be related to specific transcription factors activation under glycolytic condition. On one hand, we compared the promoter region, of viperin and OAS1 and on the other hand the promoter region of ISG12, ISG15 and ISG54, using PROMO tool based on TRANSFAC 8.3, looking for potential transcription factor binding sites. As represented, we determine three potential transcription factors that are specific for viperin and OAS1: STAT5A, NF-Y and E2F-1.

Figure 7 – Bidirectional ISGs expression is based on differential metabolic states. In cells relying on OXPHOS, antiviral response mounting is related to more functional mitochondria, leading to higher expression of ISGs. On the contrary, in cells relying on glycolysis, less efficient interferon signaling is associated with less functional mitochondria and consequently lower ISGs expression. Viperin and OAS1 escape this process and are more expressed in glycolysis-dependent cells, independently from interferon β.

Table 1 – List of qPCR primers

Gene	Forward primer	Reverse primer
RNA polymerase II	5'-GAGAGCGTTGAGTTCCAGAACC-3'	5'-TGGATGTGTGCGTTGCTCAGCA-3'
18S ribosomal RNA	5’-AGCCTGCGGCTTAATTTGAC-3’	5’-CAACTAAGAACGGCCATGCA-3’
ISG56	5’-GCAGCCAAGTTTTACCGAAG-3’	5’-CACCTCAAATGTGGGCTTTT-3’
ISG54	5’-CTGGTCACCTGGGGAAACTA-3’	5’- GAGCCTTCTCAAAGCACACC-3’
ISG15	5’-AGATCACCCAGAAGATCGGC-3’	5’-GAGGTTCGTCGCATTTGTCC-3’
ISG12	5'-CGTCCTCCATAGCAGCCAAGAT-3'	5'-ACCCAATGGAGCCCAGGATGAA-3'
IRF1	5'-GAGGAGGTGAAAGACCAGAGCA-3'	5'-TAGCATCTCGGCTGGACTTCGA-3'
Viperin	5’-GATGTTGGTGTAGAAGAAGC-3’	5’-CCAATCCAGCTTCAGATCAG-3’
OAS1	5’-CATGCAAATCAACCATGCCA-3’	5’-ACAACCAGGTCAGCGTCAGATC-3’
CMPK2	5’-CCAGGTTGTTGCCATCGAAG-3’	5’-CAAGAGGGTGGTGACTTTAAGAG-3’
lncRNA-NRIR	5’-CCACCCCCACGAAGAAATTATATATC-3’	5’-GTTAGAGGTGTCTGCTGCAATAATC-3’
IFN-β	5’-CTTGGATTCCTACAAAGAAGCAGC-3’	5’-TCCTCCTTCTGGAACTGCTGCA-3’

Table 2 – List of antibodies used for Western Blot

Target	Reference	Dilution
Rabbit anti-ISG15	MA5-29371 (Invitrogen)	1:1000
Mouse anti-ISG56	MA5-25050 (Invitrogen)	1:1000
Mouse anti-Viperin	MABF106 (Sigma-Aldrich)	1:1000
Mouse anti-IFN-β	AB_2122765 (Biolegend)	1:1000
Rabbit anti-pSTAT2	07-224 (Sigma-Aldrich)	1:1000
Rabbit anti-β-Tubulin	AC008 (ABclonal)	1:1000
Mouse 4G2 (panflaviviral anti-E)	RD Biotech	1:1000
Goat anti-rabbit immunoglobulin-HRP	AB_2313567 (Jackson ImmunoResearch)	1:5000
Goat anti-mouse immunoglobulin-HRP	AB_10015289 (Jackson ImmunoResearch)	1:5000

Table 3 – List of antibodies used for immunofluorescence

Target	Reference	Dilution
Mouse anti-TOM20	sc-17764 (Santa Cruz)	1:200
Mouse anti-IFN-β	AB_2122765 (Biolegend)	1:200
Rabbit anti-STAT2	sc-22816 (Santa Cruz)	1:200
Donkey anti-mouse Alexa 488	ab150105 (abcam)	1:750
Donkey anti-rabbit Alexa 488	ab150073 (abcam)	1:750

Figure 1

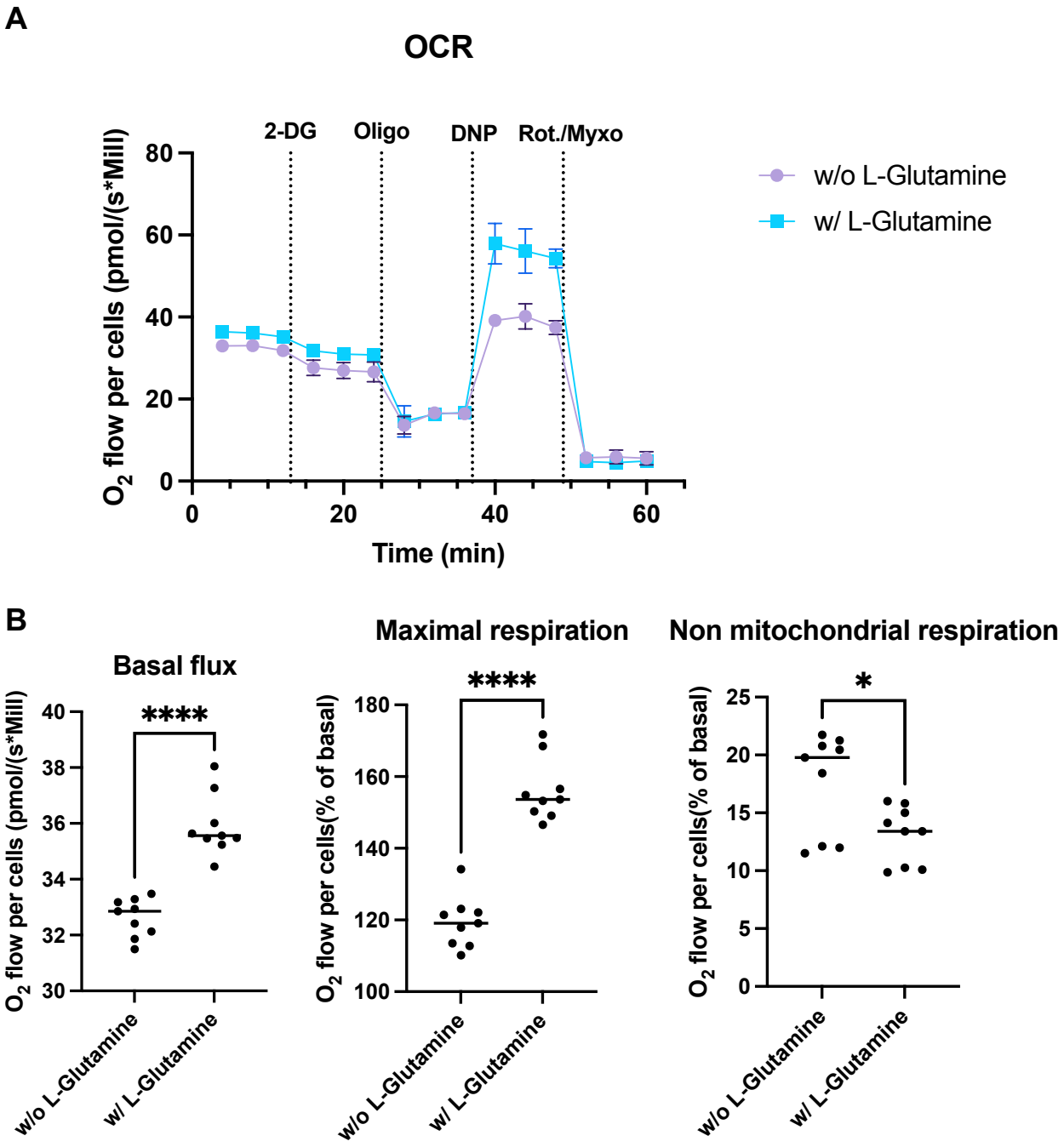
A
OCR
2-DG
Oligo
DNP
Rot./Myxo
O_2 flow per cells (pmol/(s*Mill))
80
60
40
20
0
0
20
40
60
Time (min)
w/o L-Glutamine
w/ L-Glutamine
B
Basal flux
****
O_2 flow per cells (pmol/(s*Mill))
40
38
36
34
32
30
w/o L-Glutamine
w/ L-Glutamine
Maximal respiration
****
O_2 flow per cells(% of basal)
180
160
140
120
100
w/o L-Glutamine
w/ L-Glutamine
Non mitochondrial respiration
*
O_2 flow per cells(% of basal)
25
20
15
10
5
0
w/o L-Glutamine
w/ L-Glutamine

Figure 2

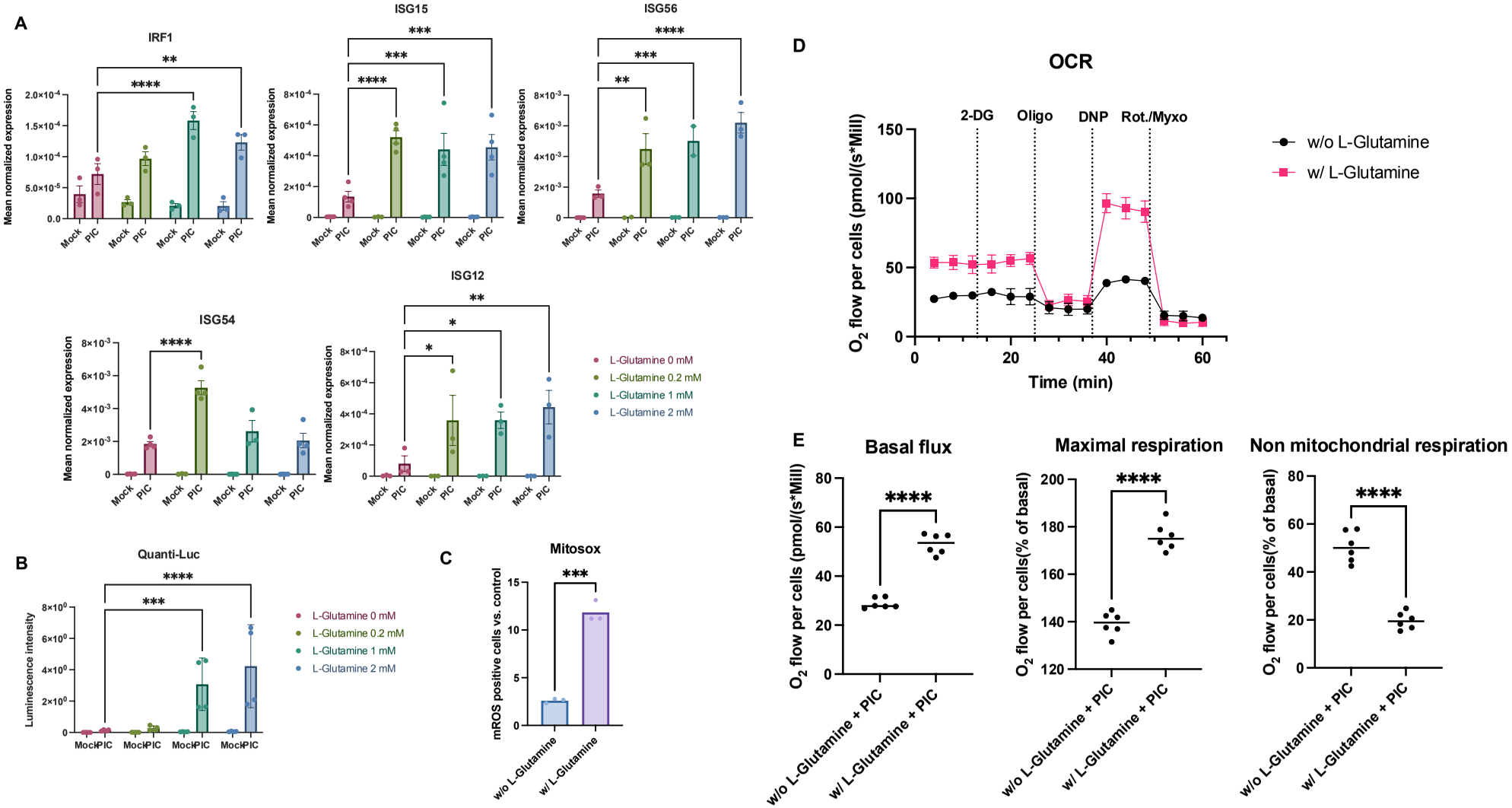
A
IRF1
ISG15
ISG56
ISG54
ISG12
Mean normalized expression
Mock
PIC
L-Glutamine 0 mM
L-Glutamine 0.2 mM
L-Glutamine 1 mM
L-Glutamine 2 mM
B
Quanti-Luc
Luminescence intensity
C
Mitosox
mROS positive cells vs. control
w/o L-Glutamine
w/ L-Glutamine
D
OCR
2-DG
Oligo
DNP
Rot./Myxo
O2 flow per cells (pmol/(s*Mill))
Time (min)
E
Basal flux
Maximal respiration
Non mitochondrial respiration
O2 flow per cells(% of basal)
w/o L-Glutamine + PIC
w/ L-Glutamine + PIC

Figure 3

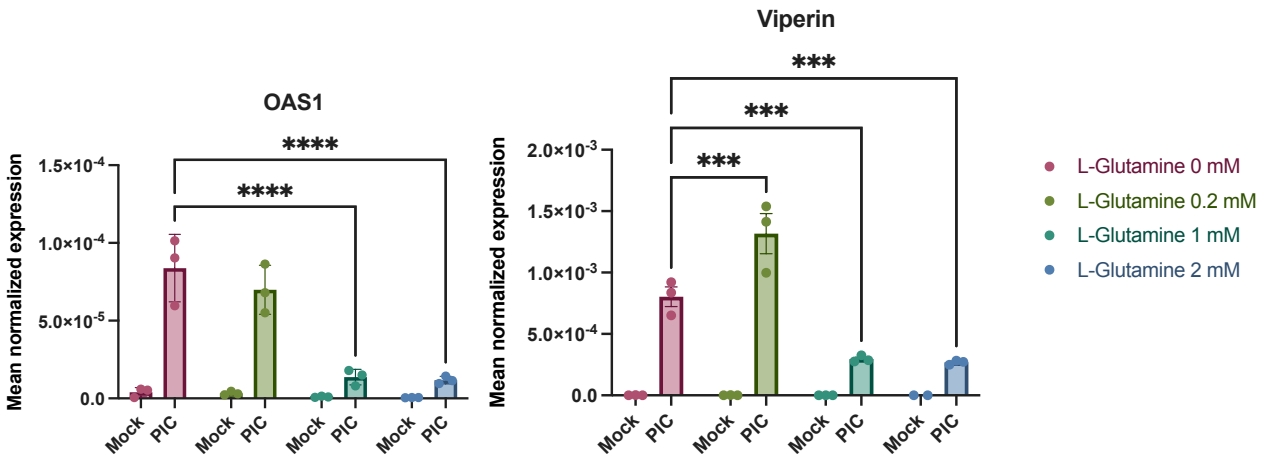
OAS1
Mean normalized expression
1.5×10-4
1.0×10-4
5.0×10-5
0.0
****
****
Mock
PIC
Mock
PIC
Mock
PIC
Mock
PIC
Viperin
Mean normalized expression
2.0×10-3
1.5×10-3
1.0×10-3
5.0×10-4
0.0
***
***
***
Mock
PIC
Mock
PIC
Mock
PIC
Mock
PIC
L-Glutamine 0 mM
L-Glutamine 0.2 mM
L-Glutamine 1 mM
L-Glutamine 2 mM

Figure 4

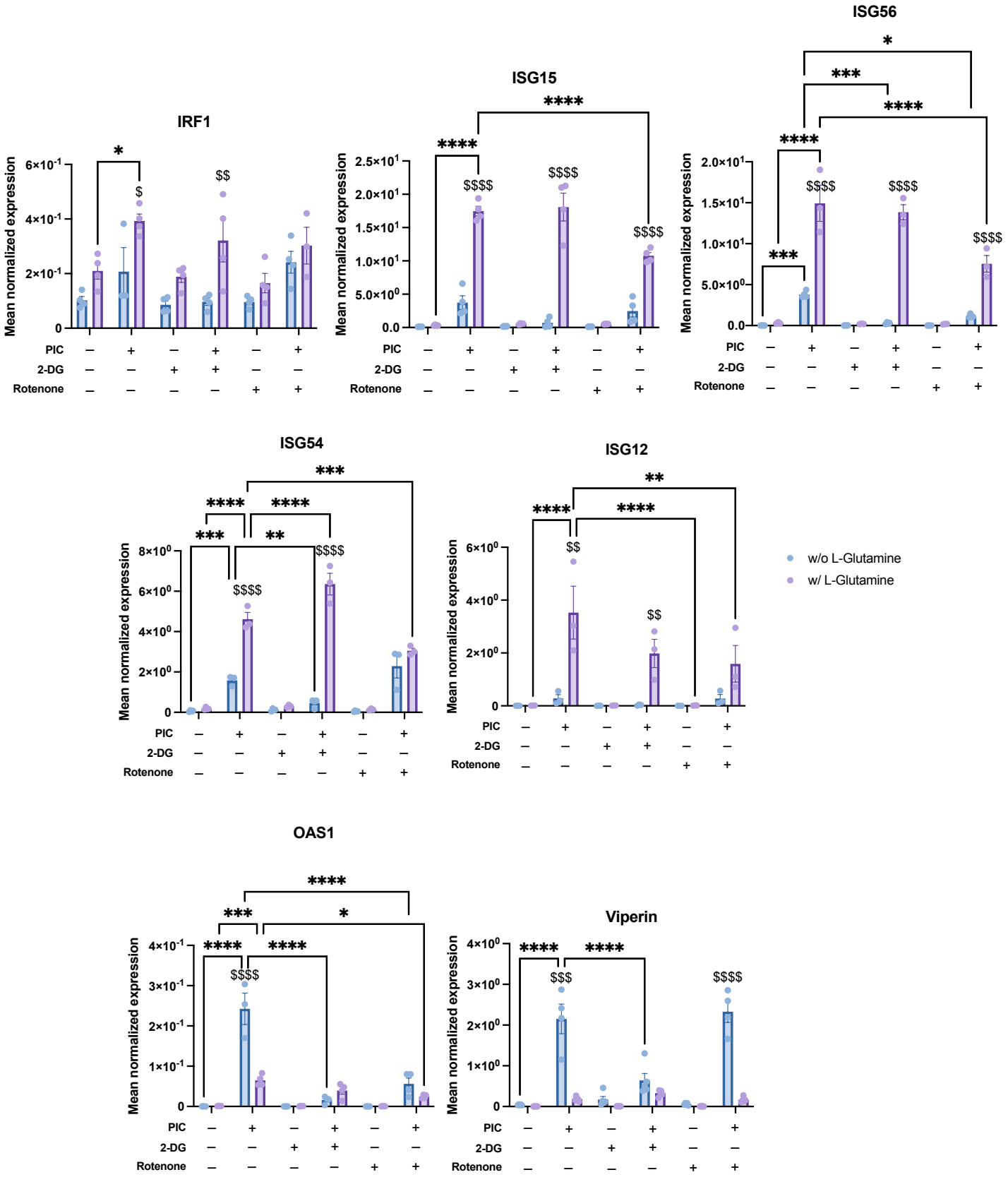
IRF1
ISG15
ISG56
ISG54
ISG12
OAS1
Viperin
Mean normalized expression
PIC
2-DG
Rotenone
w/o L-Glutamine
w/ L-Glutamine

Figure 5

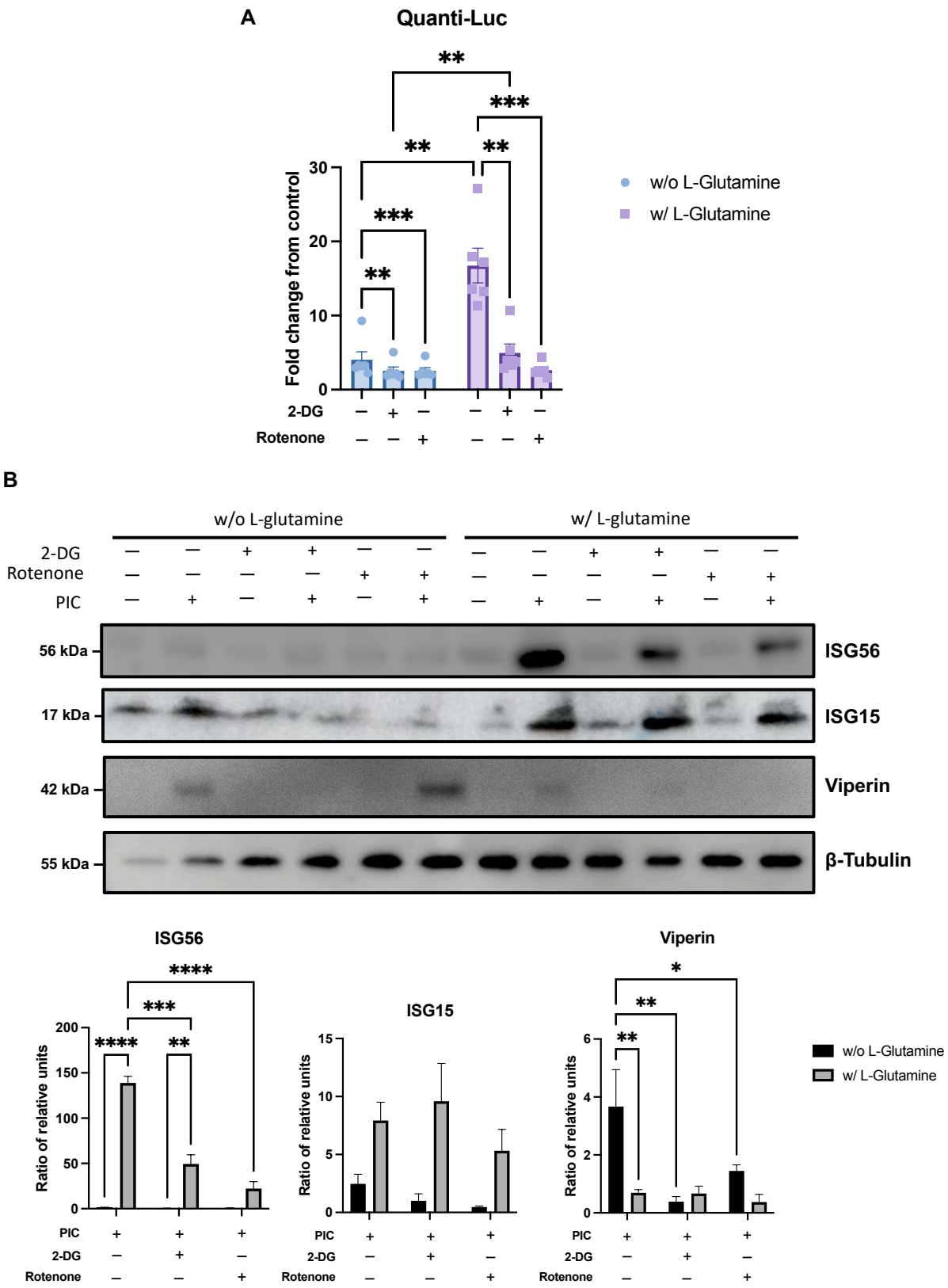
A
Quanti-Luc
Fold change from control
30
20
10
0
**
***
**
**
***
**
w/o L-Glutamine
w/ L-Glutamine
2-DG
Rotenone
B
w/o L-glutamine
w/ L-glutamine
2-DG
Rotenone
PIC
56 kDa
17 kDa
42 kDa
55 kDa
ISG56
ISG15
Viperin
β-Tubulin
ISG56
Ratio of relative units
200
150
100
50
0
****
***
****
**
ISG15
15
10
5
0
Viperin
6
4
2
0
*
**
**
w/o L-Glutamine
w/ L-Glutamine
PIC
2-DG
Rotenone

Figure 6

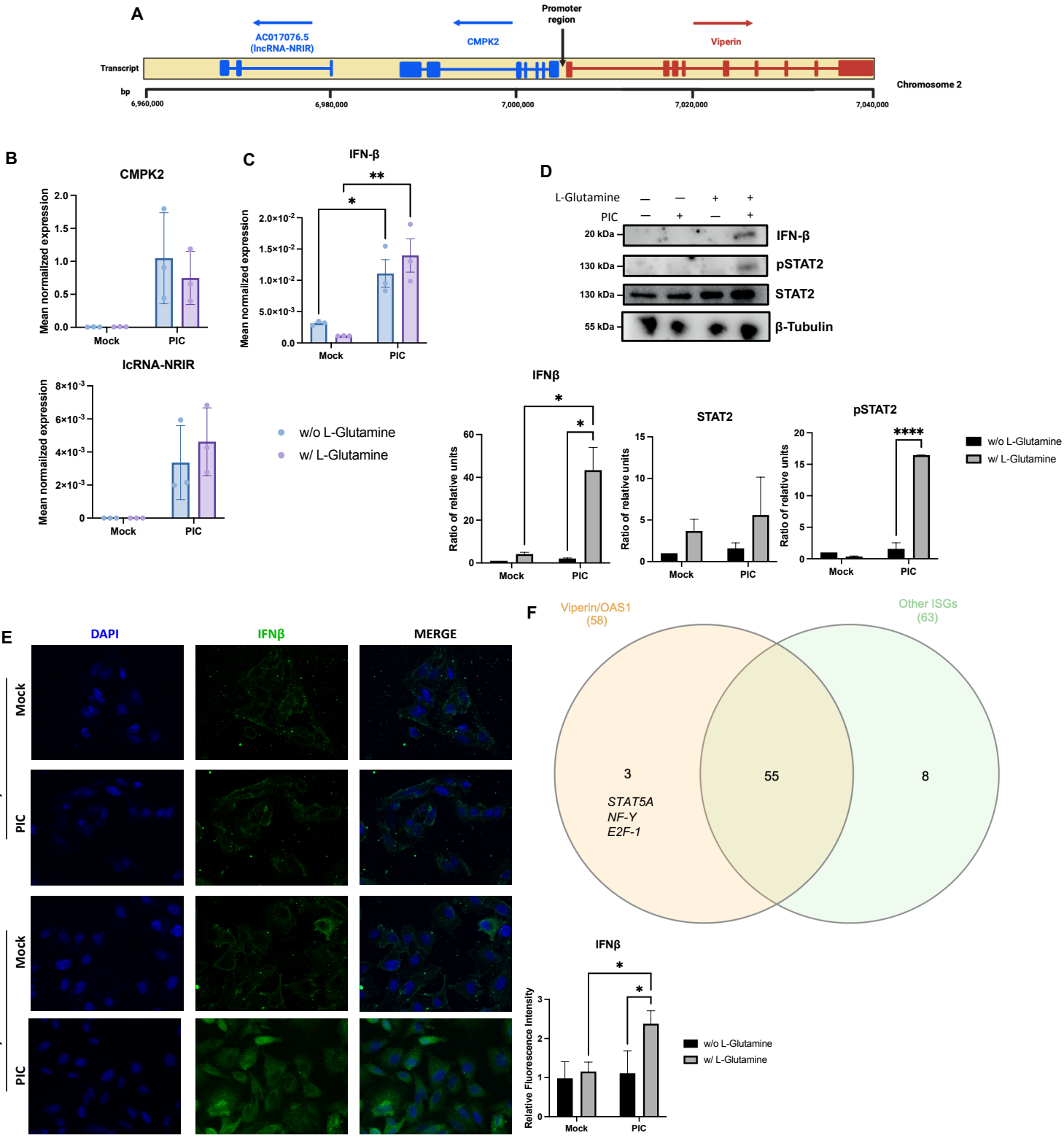
A
Promoter region
AC017076.5 (lncRNA-NRIR)
CMPK2
Viperin
Transcript
Chromosome 2
bp
6,960,000
6,980,000
7,000,000
7,020,000
7,040,000
B
CMPK2
Mean normalized expression
Mock
PIC
lcRNA-NRIR
w/o L-Glutamine
w/ L-Glutamine
C
IFN-β
D
L-Glutamine
PIC
20 kDa
130 kDa
55 kDa
IFN-β
pSTAT2
STAT2
β-Tubulin
IFNβ
STAT2
pSTAT2
Ratio of relative units
E
DAPI
IFNβ
MERGE
w/o L-Glutamine
w/ L-Glutamine
Mock
PIC
F
Viperin/OAS1 (58)
Other ISGs (63)
3
55
8
STAT5A
NF-Y
E2F-1
IFNβ
Relative Fluorescence Intensity

Figure 7

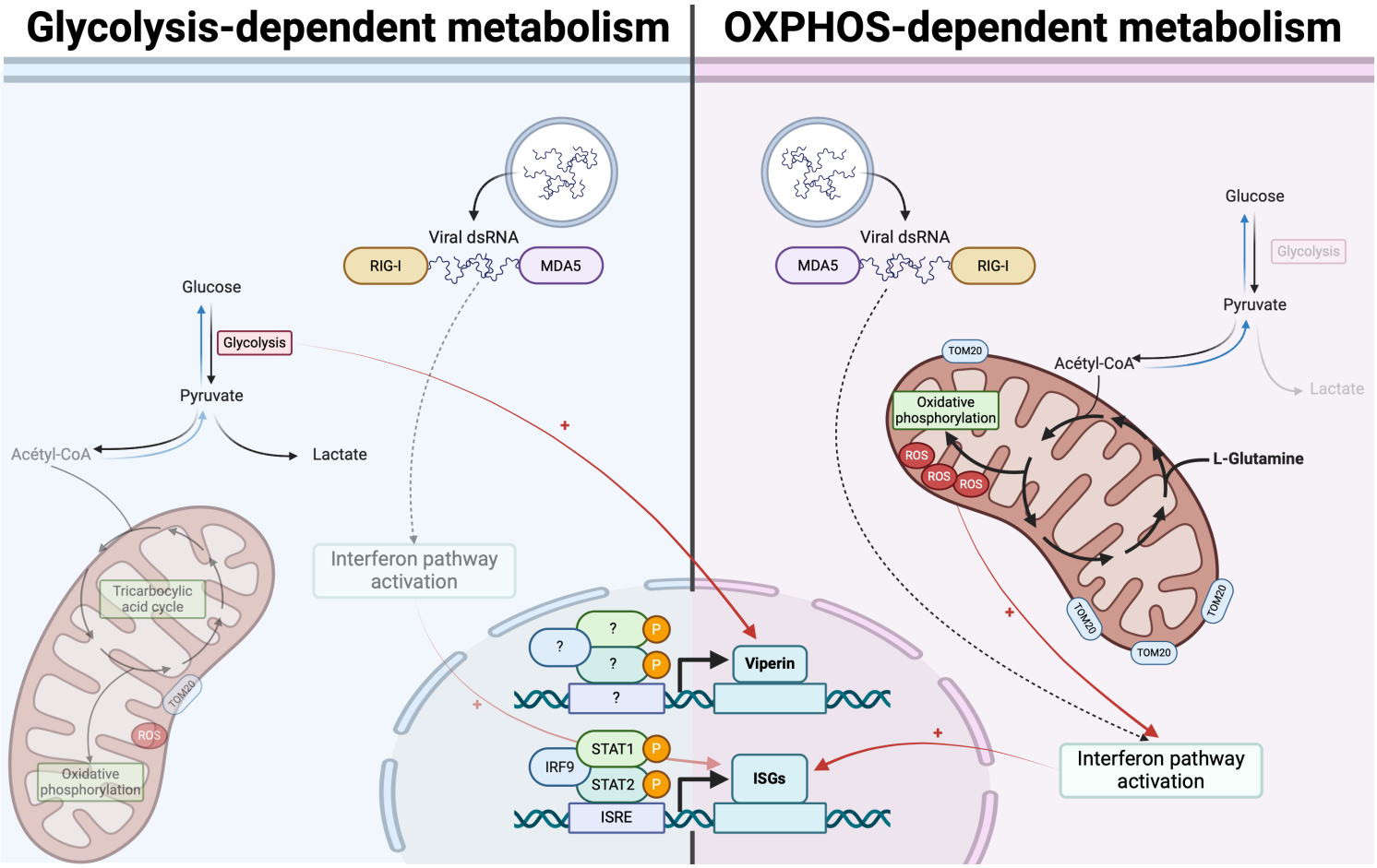
Glycolysis-dependent metabolism
OXPHOS-dependent metabolism
Viral dsRNA
RIG-I
MDA5
Glucose
Glycolysis
Pyruvate
Acétyl-CoA
Lactate
Tricarbocylic acid cycle
TOM20
ROS
Oxidative phosphorylation
Interferon pathway activation
?
P
Viperin
STAT1
STAT2
IRF9
ISGs
ISRE
L-Glutamine

Figure S1

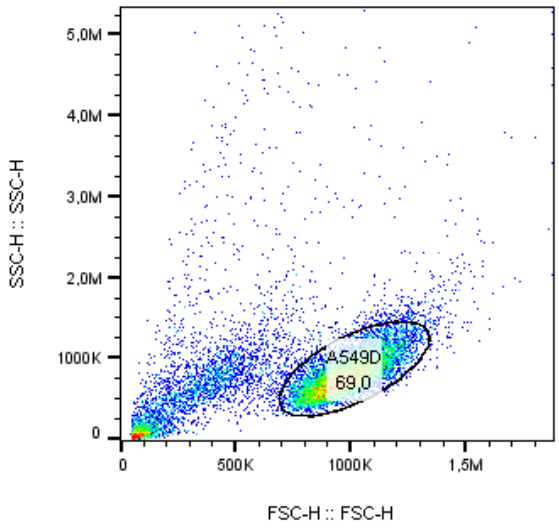

Control A549D + DMSO

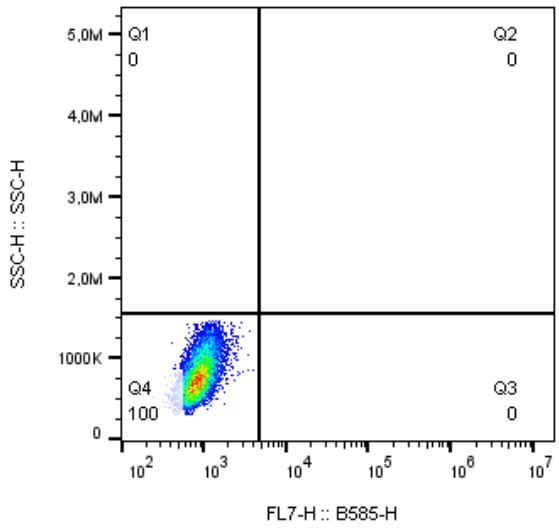

w/o L-Glutamine + Mitosox

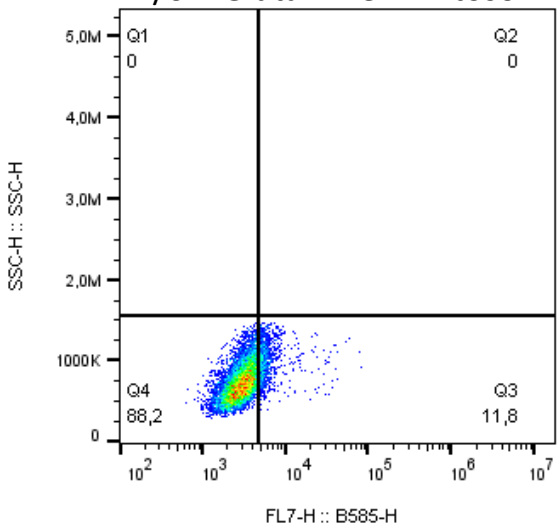

w/ L-Glutamine + Mitosox

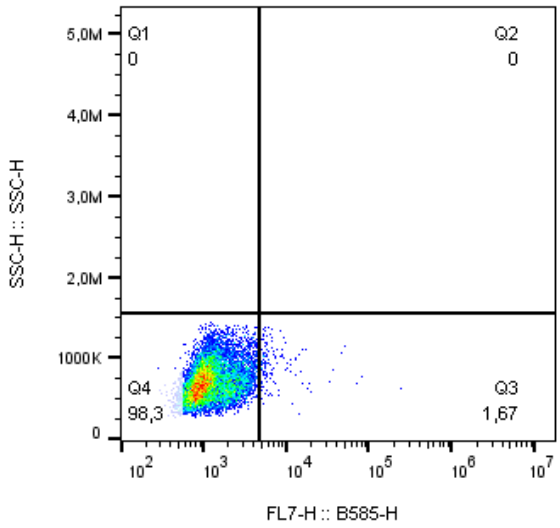

+ Poly:IC

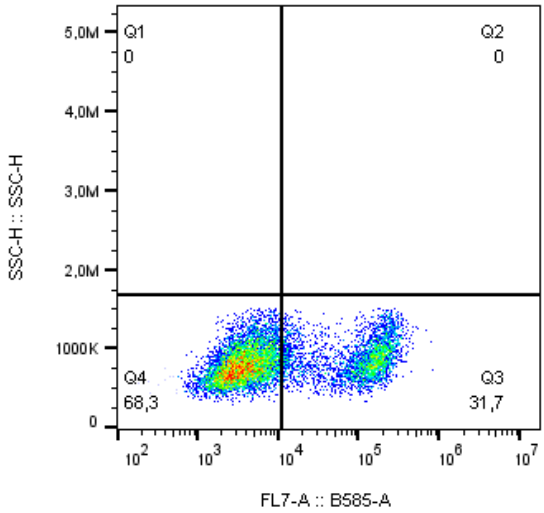

+ Poly:IC

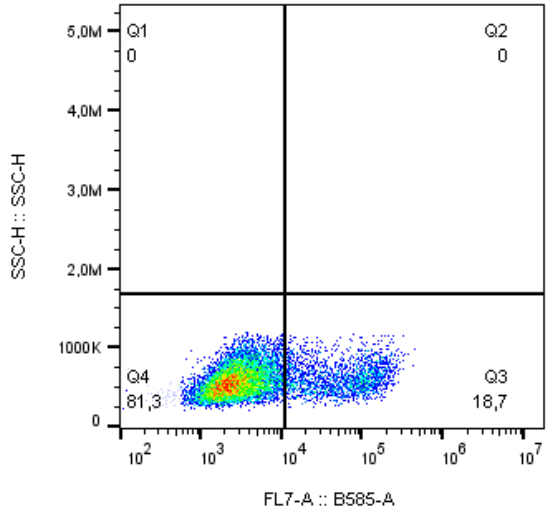

Figure S2

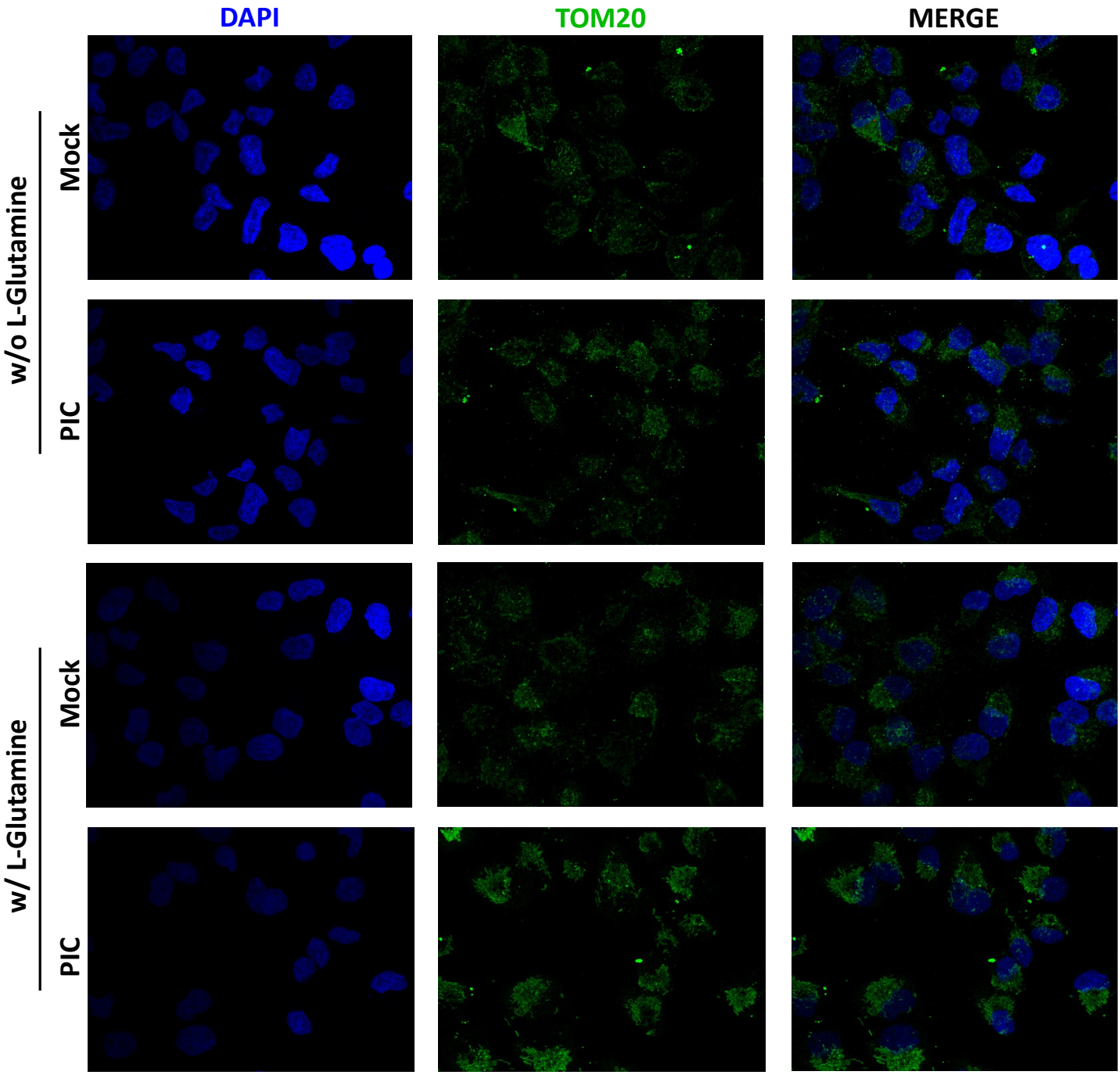
DAPI
TOM20
MERGE
w/o L-Glutamine
Mock
PIC
w/ L-Glutamine
Mock
PIC

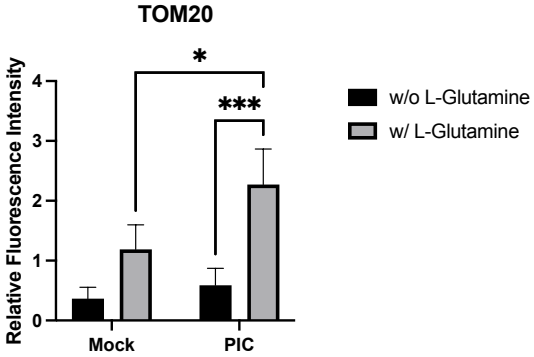
TOM20
Relative Fluorescence Intensity
0
1
2
3
4
*
***
Mock
PIC
w/o L-Glutamine
w/ L-Glutamine

Figure S3

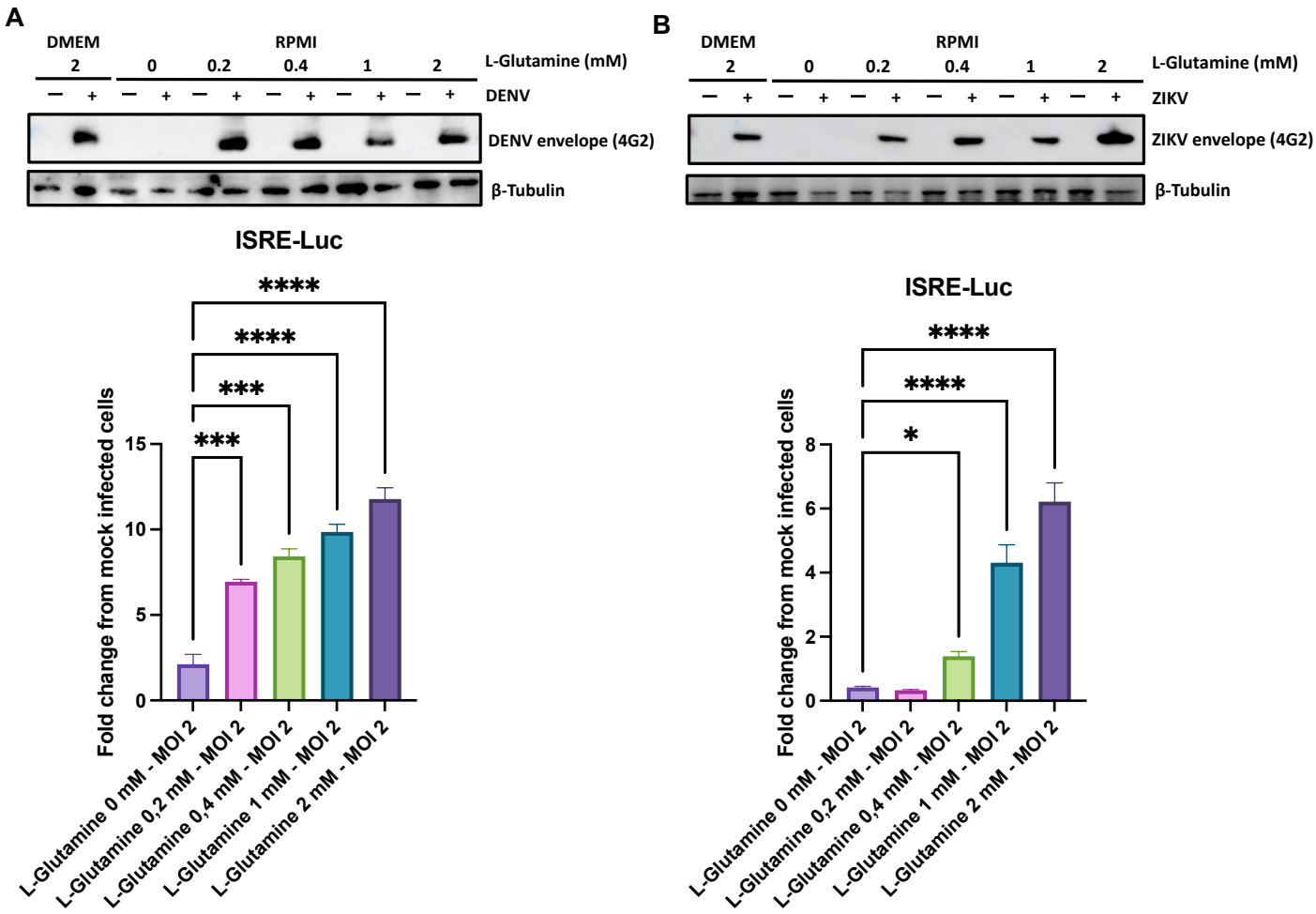
A
DMEM
RPMI
2
0
0.2
0.4
1
2
L-Glutamine (mM)
DENV
DENV envelope (4G2)
β-Tubulin
ISRE-Luc
Fold change from mock infected cells
L-Glutamine 0 mM - MOI 2
L-Glutamine 0,2 mM - MOI 2
L-Glutamine 0,4 mM - MOI 2
L-Glutamine 1 mM - MOI 2
L-Glutamine 2 mM - MOI 2
B
ZIKV
ZIKV envelope (4G2)

Figure S4

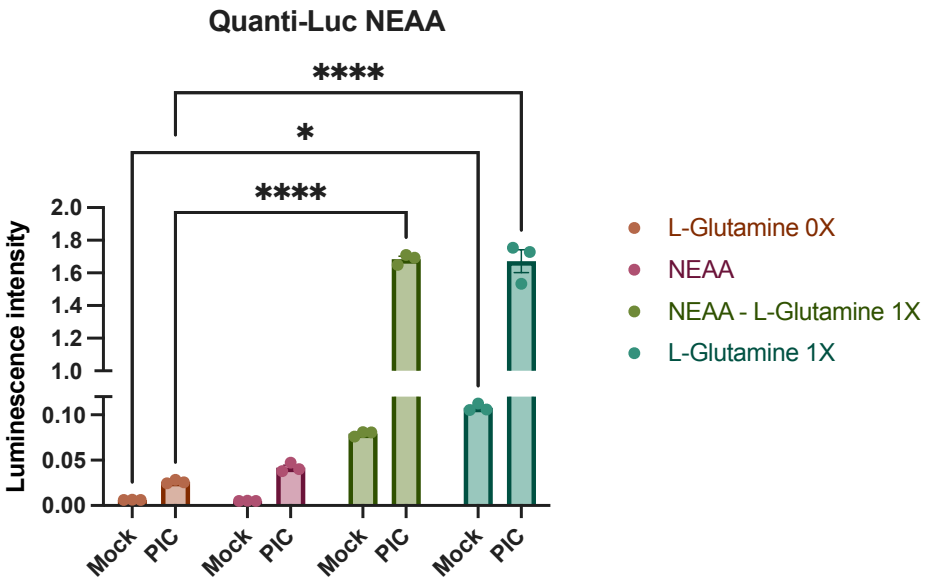
Quanti-Luc NEAA
****
*
****
Luminescence intensity
2.0
1.8
1.6
1.4
1.2
1.0
0.10
0.05
0.00
Mock
PIC
Mock
PIC
Mock
PIC
Mock
PIC
L-Glutamine 0X
NEAA
NEAA - L-Glutamine 1X
L-Glutamine 1X

Figure S5

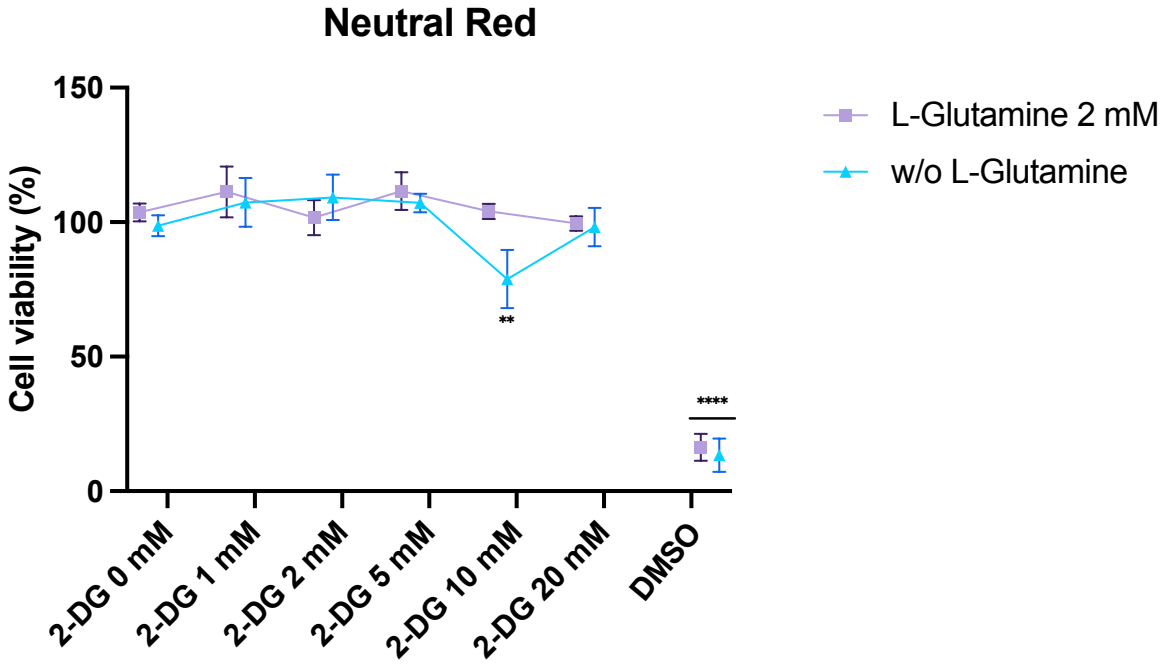
Neutral Red
Cell viability (%)
150
100
50
0
**
****
2-DG 0 mM
2-DG 1 mM
2-DG 2 mM
2-DG 5 mM
2-DG 10 mM
2-DG 20 mM
DMSO
L-Glutamine 2 mM
w/o L-Glutamine

Supplementary material

Figure S1 – Gating strategy for flow cytometry-based MitoSOX™ Red assay. Living $A549^{Dual}$ were stained with MitoSOX™ Red at a final concentration of 5 µM, after a stimulation of 6 hour with PIC 0.25 $\mu g \cdot mL^{-1}$. Cells were gated by using forward scatter versus side scatter and mitochondrial ROS induction was assessed based on positive signal in PE channel.

Figure S2 – Increased OXPHOS is associated with higher mitochondrial TOM20 labeling. TOM20 expression was assessed by immunofluorescence in $A549^{Dual}$, grown in RPMI 2 $g \cdot L^{-1}$ glucose, supplemented or not with 2 mM, using PIC 0.25 $\mu g \cdot mL^{-1}$. These images are representative of three independent experiments. Error bars represent standard deviation from three independent experiments. * $p<0.0332$; *** $p<0.0002$.

Figure S3 – Effect of glutamine on the establishment of the antiviral response during flaviviral infection. $A549^{Dual}$ grown in RPMI 2 $g \cdot L^{-1}$ glucose, supplemented or not with 2 mM L-glutamine, were infected with Dengue Virus (A) and Zika Virus (B) at MOI 2 respectively during 48h and 24h. The infection was confirmed by immunodetection of the viral envelope protein (E) using a pan-flaviviral anti-E antibody (mouse 4G2). These images are representative of three independent experiments. Evaluation of IRF pathway activation in response to infection was achieved by measuring activity of secreted Lucia luciferase, using QUANTI-Luc substrate. Results are expressed as fold change in emitted luminescence intensity from mock infected cells. Error bars represent standard deviation from three independent experiments. * $p<0.0332$; ** $p<0.0021$; *** $p<0.0002$; **** $p<0.0001$.

Figure S4 – Antiviral response upregulation is independent of non-essential amino acids. Evaluation of IRF pathway activation in response to PIC 0.25 $\mu g \cdot mL^{-1}$ stimulation of $A549^{Dual}$ grown in RPMI 2 $g \cdot L^{-1}$ glucose supplemented with either or both non-essential amino acids – NEAA and 2 mM L-glutamine, was achieved by measuring activity of secreted Lucia luciferase, using QUANTI-Luc substrate 24 hours after treatment. Results are expressed as emitted luminescence intensity. Error bars represent standard deviation of three independent experiments. *$p<0.0332$; ** $p<0.0021$; *** $p<0.0002$; **** $p<0.0001$.

Figure S5 – 2-deoxyglucose exerts no cytotoxic effect. We treated $A549^{Dual}$ with 2-deoxyglucose with concentrations ranging from 1 mM to 20 mM for 24 hours. We then evaluated the impact of these different concentrations on cell viability by neutral red assay.